

## In this issue:

New clues to petroleum prospectivity, Philippines .....	1
Palaeomagnetism "whopper", McArthur Basin .....	2
Geometry of Gunnedah Basin and New England Orogen.....	3
Position-located whole-rock geochemistry.....	4
Contacts and structure, Hinckley Gabbro, Giles Complex, W.A. . .	6
Chinese earthquakes to rock Australian buildings .....	9
Chronology, tectono-thermal, crust-forming events, Musgrave Block .....	9
Aquifers at risk .....	11
Salt lake dynamics, wastewater disposal .....	12
New mapping, Bathurst .....	13
Sequence stratigraphy, Bowen and Surat Basin, Taroom region	15
Magnetic anomaly map of Australia .....	16

## New clues to petroleum prospectivity of offshore Philippines Basins with AGSO surface geochemical (DHD) techniques

The AGSO recently (March/April 1992) collected both seismic and bottom-water 'geochemical sniffer' (Direct Hydrocarbon Detection, i.e. DHD) data from the offshore Philippines. This project is being conducted by AGSO for the Philippines Office of Energy Affairs with funding from the Australian International Development Assistance Bureau. Approximately 2750 line-km of seismic and 5000 line-km of bottom-water geochemical data were obtained from four areas: northeast Palawan, Cuyo Platform, Tayabas Bay, and Ragay Gulf.

The bottom-water geochemical data were collected using the continuous geochemical profiling capability installed on Rig Seismic (BMR Research Newsletter, 10, 12-13, 1989), deployed amidships from a large A-frame to allow simultaneous acquisition of geochemical and conventional seismic data. This bottom-water DHD technique seeks evidence of thermogenic hydrocarbons in seawater that have migrated from sub-seafloor hydrocarbon accumulations or petroleum source rocks, through faults in the overlying sedimentary strata, into bottom-waters on the continental shelf. Preliminary results are:

- Several weak (less than two-fold typical background concentrations) bottom-water hydrocarbon anomalies were found in the northeast Palawan area.

- No significant anomalies were found in the Cuyo Platform and Tayabas Bay areas.
- Many strong (greater than ten-fold typical background concentrations), significant bottom-water hydrocarbon anomalies were discovered in the Ragay Gulf area.

An example of the DHD data (survey line 109/44) in the Ragay Gulf is illustrated in Figure 1, depicting a moderate-to-strong (hydrocarbon concentrations approaching an order of magnitude above background levels) anomaly in both THC (total hydrocarbons) and methane concentrations near 100 ppm. This anomaly was accompanied by increases in ethane, propane and butane an order of magnitude above background. The anomaly extends for about 10 shot-points, or about 3 km on the seafloor.

Field observations showed two types of hydrocarbon anomalies in bottom-waters. **Type I** anomalies are characterised by high concentrations of methane, ethane and propane, with traces of butanes and pentanes. Hydrocarbon wetness values [% wetness =  $(C_2 + C_3 + C_4) / (C_1 + C_2 + C_3 + C_4) \times 100$ ] are 1-1.5%. **Type II** anomalies are characterised by high concentrations of methane only, with traces of ethane. Hydrocarbon wetness values are < 0.5 %.

The differences between these two types of anomalies are shown in cross-plots of percent hydrocarbon wetness versus methane concentration (Fig.2). The trends in these plots may be used to predict the hydrocarbon 'source' (dry gas, gas-condensate, liquids-prone), which produces the bottom-water hydrocarbon anomalies. For example, increasing wetness with increasing methane (Type I anomalies) suggest the bottom-water hydrocarbons are 'sourced' from gas/condensate source rocks or accumulations. Decreasing wetness with increasing methane (Type II) anomalies are indicative of either dry thermogenic gas or biogenic hydrocarbons.

These field-data are being edited and processed. Carbon isotopic analyses, in conjunction with the molecular compositional data, will be used to distinguish the possible 'source' of bottom-water anomalies, particularly whether the 'dry' gas anomalies are of a thermogenic or biogenic origin.

The geochemical data will be integrated with the seismic data (providing clues to hydrocarbon migration pathways in the areas

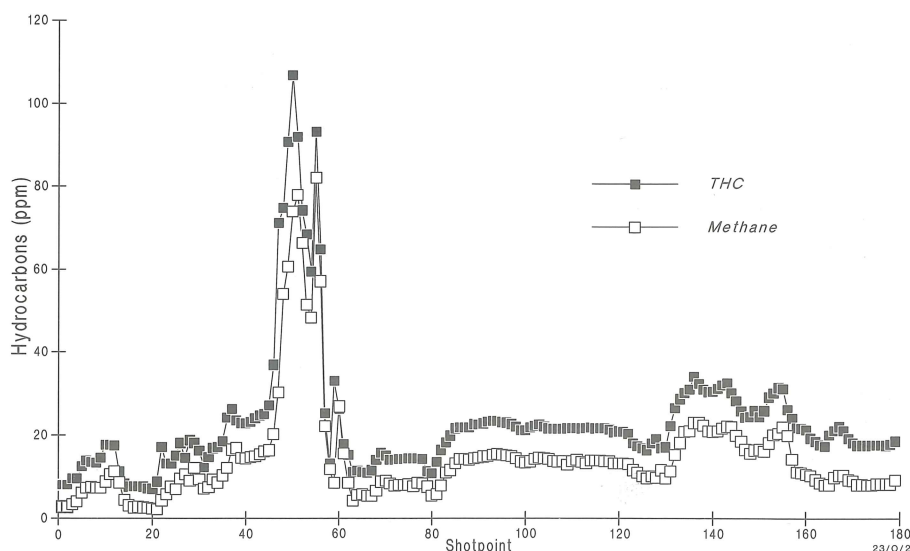
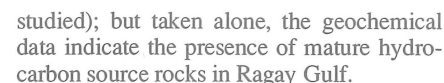


Fig. 1. Total hydrocarbons (THC) and methane along survey line 109/44 in the Ragay Gulf.





*For further information, contact J.H. Bishop, D.T. Heggie, C.S. Lee or D. Evans, Program in Marine Geoscience and Petroleum Geology, AGSO.*

**Fig. 2. Methane versus percent hydrocarbon wetness, illustrating the two Types of anomalies found in the Ragay Gulf.**

## Palaeomagnetism delivers a “whopper” on the southeastern McArthur Basin

nihilated the original remanence. Another difficulty with Precambrian magnetostratigraphy is the lack of appropriate markers, such as key fossils, to ensure that the polarity patterns being compared for correlation purposes actually represent the same set of reversals. The McArthur Basin was selected as its sequences appear to be unmetamorphosed, thus avoiding a major cause of Precambrian overprinting. Integral to the study was the construction of a detailed polar wander path allowing the use, in the absence of fossils, of remanence directions to pair up corresponding reversal patterns for detailed correlation.

Based on over 1800 samples, this is the most extensive study known of any sedimentary basin. It yielded twelve primary poles, increasing the Proterozoic palaeomagnetic database for Australia by over 30%. Ten of the poles define a path segment that spans ~100 m.y. and is centred at ~1650 Ma (Fig. 1). These poles show the basin to have been in low to middle latitudes throughout its depositional history. The measurements yield also ten overprint poles, which plot on the path in three main groups:

- The oldest group lies on the ~1700 Ma path segment, and appears to record a widespread metasomatism recognised

**Fig. 2. Composite reversal column for the McArthur Basin. Grey indicates uncertain polarity.**

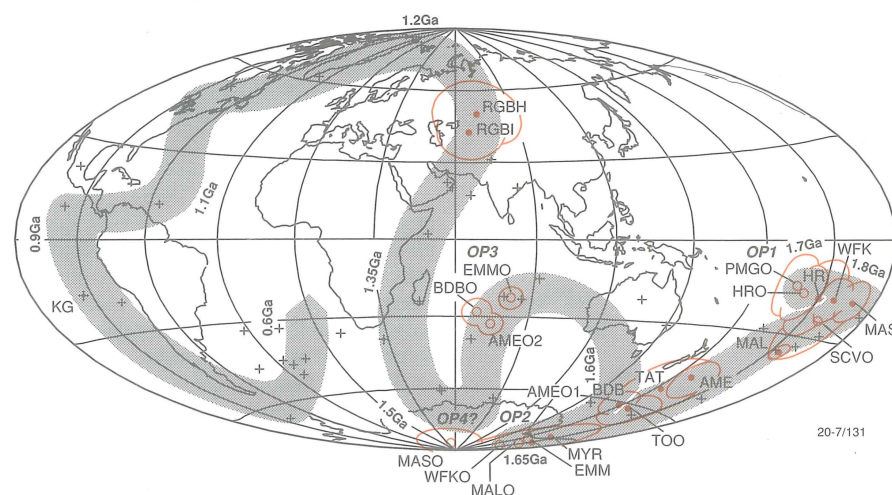
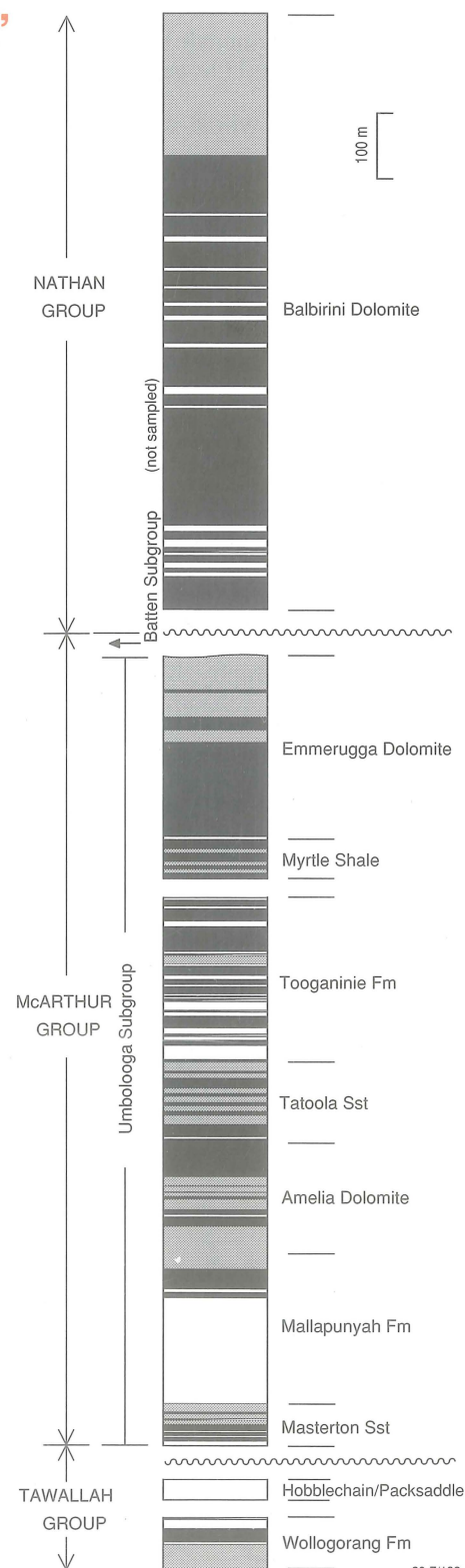


**Fig. 1.** Early to late Proterozoic polar wander path for Australia. Poles obtained are shown with 95% confidence circles (in colour); those shown with open symbols are due to overprints.





also in other geological studies.

- The second group, comprising overprints found at sampling sites near two prominent faults, appears to be due to hydrothermal activity at ~1650 Ma. These overprints may be the result of chemical processes associated with the formation of the giant HYC Pb-Zn-Ag deposit at McArthur River.
- The third overprint group, lying on the

~1600 Ma path segment, was found almost exclusively in carbonates, and is attributed tentatively to late diagenesis.

Some of the overprint magnetizations may indicate economically significant alteration, and specific localities will be sampled in 1992 for a follow-up geochemical study.

The results yield one of the geologically oldest reversal columns available at present (Fig. 2). This column represents parts of the

Tawallah, McArthur and Nathan Groups, spanning an accumulated stratigraphic thickness of 2000 m. Gaps exist where either overprints have destroyed the primary remanence, or the outcrop is discontinuous, or the remanence was unstable, etc. However, parts of the column are both complete and distinctive — these should be applicable to correlations in northern Australia and elsewhere.

For further information contact Dr. M. Idnurm at AGSO.

## Geometry of Gunnedah Basin and New England Orogen examined by AGSO deep seismic profile

In 1991, the AGSO *Sedimentary Basins of Eastern Australia* project, part of the National Geoscience Mapping Accord, acquired deep seismic reflection data in northern New South Wales to address

several geological problems on the origin and development of the Gunnedah and Surat basins, and their relationships with the New England and Lachlan orogens.

Prior to recording the deep seismic reflection profile across the Gunnedah Basin, a test seismic survey was carried out in May 1989 to determine optimum acquisition parameters at five sites with different surface geology.

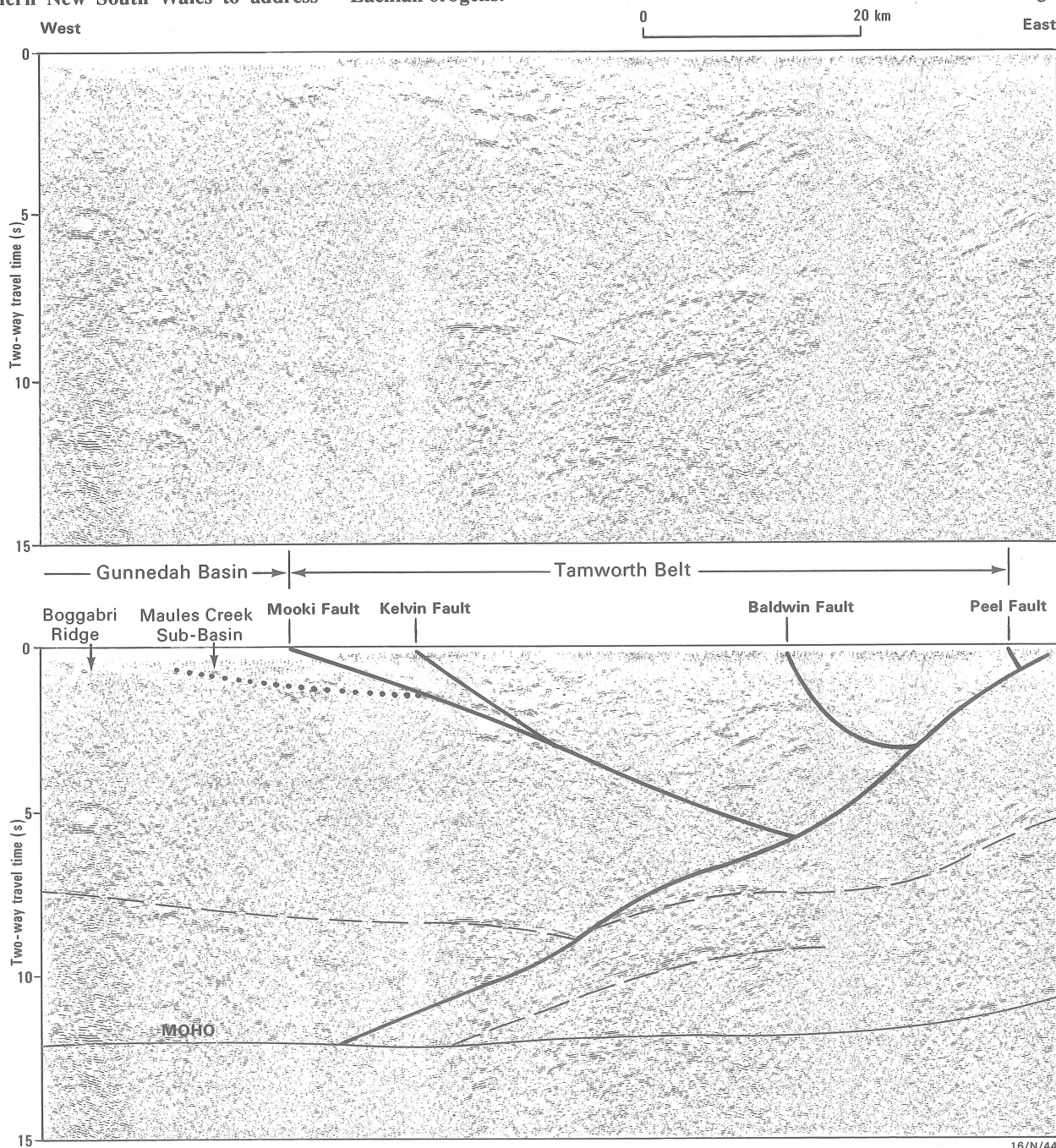


Fig. 1. Portion of unmigrated deep seismic reflection profile and preliminary geological interpretation across the eastern Gunnedah Basin and Tamworth Belt part of line BMR91.G01. Solid lines represent interpreted faults, dashed lines are strong lower crustal reflectors, and the dotted line represents the approximate base of the Maules Creek Sub-basin. Vertical scale equals horizontal scale for a velocity of  $6 \text{ km s}^{-1}$ .



Test seismic lines were 5.7 km in length (96 channels, 60 m geophone group interval, 360 m shotpoint interval). Seismic tests — including charge size and charge depth comparisons, and noise and uphole shoots — were performed at sites where additional data were required to optimise recording parameters.

In early 1991, a single, east-west oriented deep seismic reflection profile, 253 km long, was acquired at about the latitude of Boggabri, across the Gunnedah Basin and Tamworth Belt and farther east across the Peel Fault in the New England Orogen. Recording parameters to examine the relationships between basin geometry and crustal structure were: 20 seconds two-way travel time, 8-fold common mid-point (CMP), and explosive source. Routine processing of these data is complete and the results released in January 1992.

To generate a multidisciplinary geophysical data set, gravity readings were made at 360 m intervals along the seismic line. In addition, the seismic line was flown for aeromagnetics and radiometrics at flight heights of 500 ft (about 150 m) and 3000 ft (about 900 m) AGL.

Some of the scientific problems addressed by the survey (see also *BMR Record* 1990/93) included:

- the geometry of the structural units of the Gunnedah Basin,
- the geometry of the Mooki Fault (eastern margin of Gunnedah Basin),
- whether the Tamworth Belt is thin skinned, and overriding the Gunnedah Basin, and
- the geometry of the Peel Fault (the eastern margin of the Tamworth Belt) and its rela-

tionship to the Gunnedah Basin and Tamworth Belt.

In the vicinity of the seismic line, the Gunnedah Basin succession is relatively thin and consists of three sub-basins, separated by two ridges. From west to east, these are: Gilgandra Trough, Rocky Glen Ridge, West Gunnedah Sub-basin, Boggabri Ridge, and Maules Creek Sub-basin. The maximum thickness of sediment appears to be no greater than 2 km (about 1.6 s TWT) on the western side of the West Gunnedah Sub-basin. The seismic data suggest that the two ridges are not structurally controlled, and also there is no evidence of major structures that can be interpreted as bounding faults to the three sub-basins. Within the basement below the Gunnedah Basin, there is an apparent lack of dipping structures, possibly indicating that this part of the line was not affected by major extensional or contractional structures.

Within the West Gunnedah Sub-basin, an erosional unconformity is seen in places between the Late Permian Black Jack Coal Measures and conglomerates of the Triassic Digby Formation.

At the surface, the easternmost extent of the Gunnedah Basin is marked by the Mooki Fault. Although this fault is not imaged clearly in the seismic data, it appears to have a shallow dip of less than 30° to the east (Fig. 1). Thus, the Tamworth Belt has been thrust over the eastern margin of the Gunnedah Basin for at least 6 km, leading to the possibility of hidden plays beneath the westernmost part of the Tamworth Belt.

The western half of the Tamworth Belt of the New England Orogen displays a relatively simple structural geometry dominated at the

surface by the Rocky Creek Syncline, which is a hanging wall syncline above the Kelvin Thrust. A relatively thick succession occurs in the syncline (at least 5 km, 2 s TWT). To the east, the succession in the Klori Anticline appears to be over 4 km thick (1.6 s TWT). The succession in the Yarramanbully Anticline, about 10 km west of the Peel Fault is possibly much thinner. At two-way travel times of 1–4 s, the western half of the Tamworth Belt appears to be disrupted by faults that dip shallowly to the east, whereas in the eastern half of the belt its base is probably a west-dipping fault (Fig. 1). Overall, the Tamworth Belt could represent a duplex zone due to major west-directed (i.e. east-dipping) backthrusting above a deeper, west-dipping thrust zone.

Directly beneath the surface position of the Peel Fault, at a depth of about 1 km (0.4 s TWT), reflections dip moderately to the west, placing significant constraints on the geometry of the fault. Immediately east of the Peel Fault in the Tablelands Complex of the New England Orogen, a series of reflections also dip to the west. These possibly represent thrust faults within the accretionary wedge succession.

The eastern end of the line was acquired on outcrops of the Bundarra Plutonic Suite. The pluton has a shallow pancake-like shape with its floor at 6–9 km (2–3 s TWT). Although the pluton is predominantly non-reflective, a few internal structures dip to the west, confirming the results of the earlier test seismic survey.

For further information contact Russell Korsch, Kevin Wake-Dyster, or David Johnstone (Onshore Sedimentary & Petroleum Geology Program) at AGSO.

## The role of position-located whole-rock geochemical data in exploration

The essential role of stream-sediment geochemical data in regional exploration is now accepted and anomalous element abundances from specific drainage catchments are widely used to define potential areas for detailed mineral evaluation. In contrast, uses for digital, position-located, regional-scale whole-rock geochemical databases in exploration has not been recognised, possibly because many whole-rock geochemical samples were originally collected as part of more detailed petrological or ore deposit studies, and in isolation, these individual collections are generally not considered significant. However, when compiled on a regional, if not continent-wide scale, the data can have far more widespread uses than was originally intended during sample collection. New applications of position-located whole-rock geochemical data in exploration are discussed using the Australian Geological Survey Organisation (AGSO, formerly BMR) ROCKCHEM database which currently contains some 22 000 analyses from Australia (Fig. 1) from many diverse rock types, including intrusive and extrusive

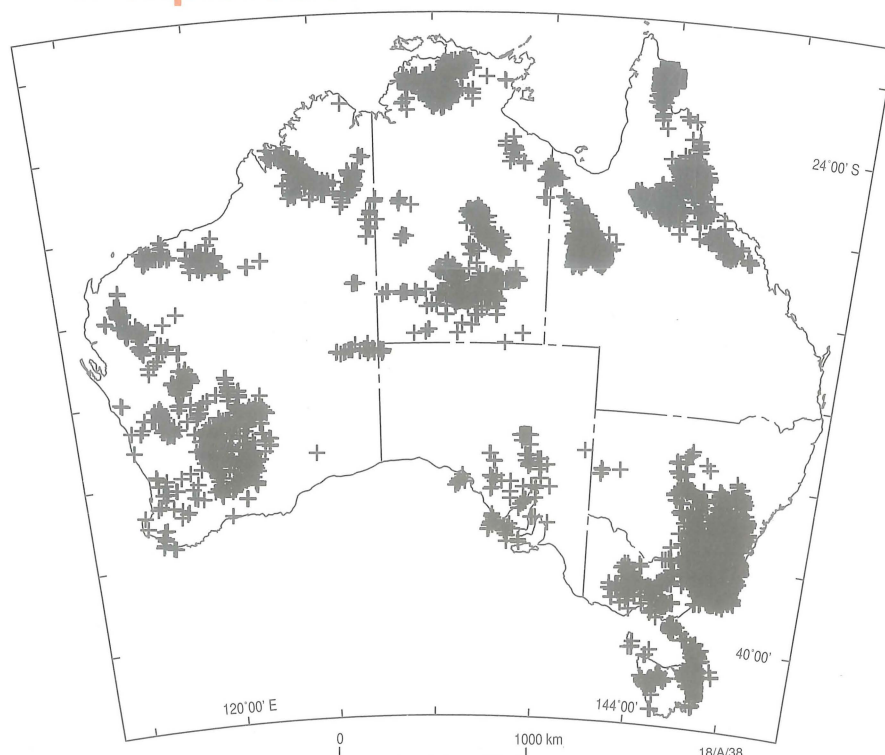


Fig. 1. Distribution of ROCKCHEM samples in Australia.



mafic, alkaline and felsic igneous rocks, sedimentary and metamorphic rocks. In addition, there are samples from several major ore deposits and their immediate environs, including the Tennant Creek gold-bismuth deposits, Alligator Rivers Uranium deposits, and the Mount Isa copper deposit.

### Potential uses for position-located whole-rock geochemical databases in mineral exploration

There are at least five potential uses:

**Stream-sediment surveys.** Using Geographic Information Systems (GIS), it is now possible to integrate whole-rock geochemical surveys with stream-sediment surveys. This can be done in one of two ways. (a) The simplest involves calculating the average value of the elements in the individual rock units that occur in a particular survey area and comparing them with the stream-sediment values. For instance, in the Kakadu area, anomalies of As, Sn, Nb, Th and U were related to the Malone Creek Granite that was also high in these elements (Cruickshank, *BMR Research Newsletter*, 12, 5-6). (b) A more complex method is to calculate the average values of certain elements in bedrock units within a particular drainage basin and then estimate the degree of enrichment/depletion in the stream sediments.

**Delineating regional alteration zones.** Many major ore deposits are surrounded by regional geochemical alteration zones which can be readily identified within the whole-rock geochemical database by the enrichment and/or depletion of elements – such as  $Al_2O_3$ ,  $K_2O$ ,  $CaO$ ,  $Na_2O$ , Th, U,  $Fe_2O_3$ ,  $FeO$  and  $CO_2$  (e.g. Coronation Hill area, NT; *BMR Research Newsletter*, 12, 1-2; Williams Batholith, Mt Isa; *BMR Research Newsletter*, 16, 13-16).

**Radiometric surveys.** Most whole-rock samples are analysed for K, Th and U; and for those regions, where the airborne radiometric data has not been previously collected, these analyses are helpful in predicting the usefulness of radiometrics in lithological discrimination.

Where both airborne radiometric and whole-rock geochemical data are available, the relative concentrations for K, Th and U for the individual geological units within the survey area can provide a rough calibration for interpreting images from the airborne radiometric surveys. Whole-rock geochemical data are almost essential for interpreting the red/green/blue (RGB) false colour image (in which potassium is assigned to the red colour gun, thorium to the green, and uranium to the blue). The simplest way to portray the geochemical data is to utilise a box-whisker plot for individual rock units within the geophysical survey area. Figure 2 is a box-whisker plot for  $K_2O$ , Th and U for each individual unit within the Kakadu survey area: the median value for each element for the whole data set

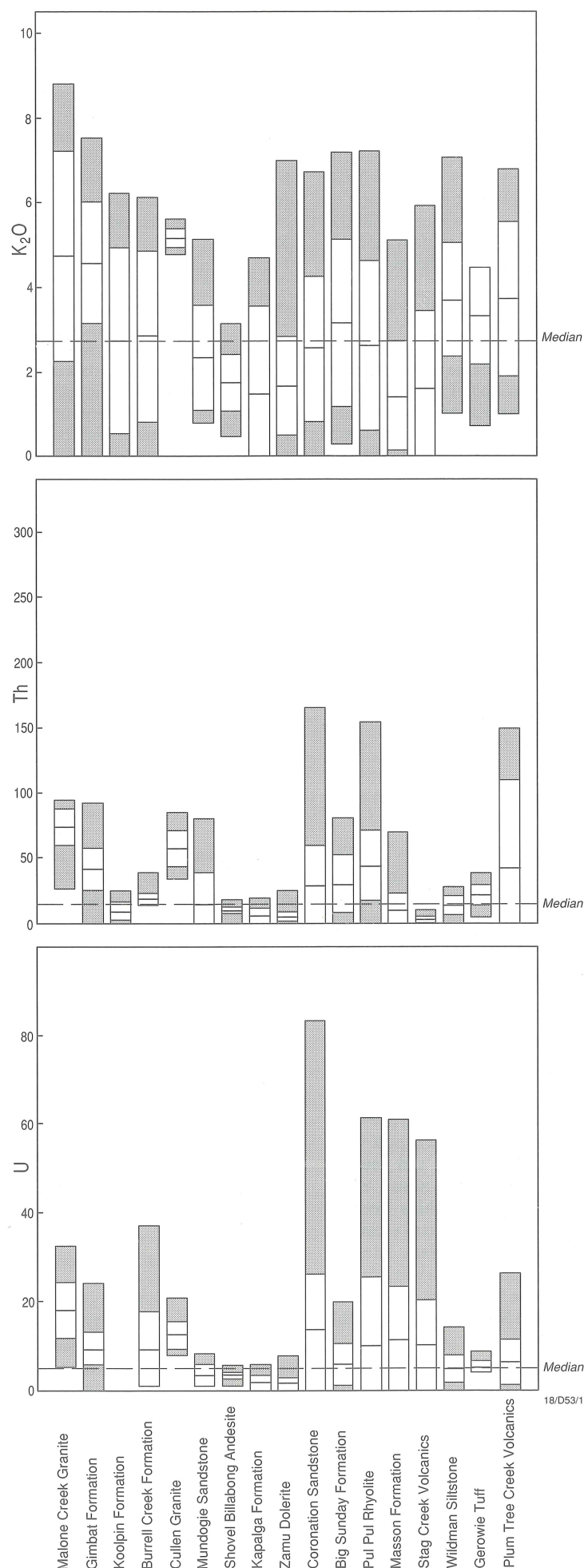


Fig. 2. Box-whisker plot of values for  $K_2O$ , Th and U for rock units in the Kakadu Geophysical Survey area. The white box shows the mean, and the range of values for samples that fall within  $\pm 1$  standard deviation, whilst the black box shows the range of values for the remaining samples. Median value is for the whole data set for each element.



is also plotted. All rocks which substantially plot above the median value for all three elements will appear white in the RGB image (e.g. felsic volcanics and granites); all units which plot below the median values will appear black. If a unit is substantially above the median value for only one element, it will take the colour for that element. For instance, the Masson Formation appears blue in the RGB image, because it has proportionally more uranium than either potassium or thorium relative to other units.

In alteration zones, where the variation of K, Th and U can be determined from whole-rock geochemical data, it is possible to then combine them with airborne radiometric data to determine the location of alteration zones. For example, in the Kakadu Conservation Zone, whole-rock geochemical data showed that all of the mines and prospects were surrounded by alteration zones up to 1 km wide in which U was depleted relative to Th. Using GIS and combining the whole-rock geochemical data with an image of  $U^2/Th$ , previously unknown areas of alteration were defined.

**Comparative study of ore deposits.** Compilations of whole-rock geochemical data from major ore deposits can be useful for comparative studies, particularly if the data is

from both surficial samples and drill core. For example, in ROCKCHEM, there is a comprehensive set of 979 analyses from the Tennant Creek ironstones from both drill core and surface samples. The former are from both ore zones and adjacent wall rocks, and thus comparative studies can be made with other areas of Australia on the type(s) of alteration associated with the Tennant Creek deposit type. ROCKCHEM also contains 480 analyses from surficial rock chip surveys of deposits in the South Alligator Mineral Field, which will enable comparison with other potential areas of Au-PGE±U unconformity-style deposits.

**Image analysis.** In some areas, if the spatial distribution of the data is dense enough and evenly distributed, images can be produced of individual elements or element ratios to highlight regions of high background values of elements, such as U and Cu.

### Future developments of whole-rock geochemical databases

There is obviously a potential use for whole-rock geochemical databases in exploration. The AGSO ROCKCHEM database will continue to expand with new data, as part of the current NGMA program. However, there is still a role for digital compilation of existing

whole-rock geochemical data, but only if it is accurately position-located. Unfortunately, many samples in theses, or other literature, are not accurately located and are useless for digital compilations, such as ROCKCHEM. Museums in universities and government geological surveys also contain position-located geochemical powders of samples from early surveys. Most of these older samples only have limited trace-element suites and many have not been adequately analysed to current standards of precision and accuracy. These powders constitute a valuable resource, particularly as many come from areas that are no longer accessible for resampling. Where possible, pre-1980 BMR rocks powders and samples are being progressively re-analysed for more accurate and comprehensive major and trace elements sets, including precious metals,  $CO_2$  and  $FeO/Fe_2O_3$ . External funding is required to accelerate (and perhaps expand) this re-analysis program, and to also compile position-located data from other non-AGSO sources. Expressions are sought from those interested in promoting this project.

*For further information contact Dr Lesley Wyborn at AGSO (Minerals and Land Use Program).*

## Contact relationships and structure of the Hinckley Gabbro and environs, Giles Complex, Western Musgrave Block, W.A.

Two key areas of the Hinckley Gabbro, which forms one of the largest intrusions within the layered basic/ultrabasic Giles Complex, have been studied to elucidate the spatial and temporal relationships between the gabbro, recrystallized gabbro and mafic granulites, older banded felsic/mafic granulites and younger charnockites, porphyritic granite, felsite/pegmatite networks and basic dykes. A resolution of the tectonic fabrics of these units allows the definition of at least seven phases of deformation, including pre-Giles Complex pure shear (D1–2), post-Giles Complex simple shear (D3), and younger mylonitic and retrograde shear zones (D4–7). The field relationships between these units and their structural elements, combined with isotopic age data, establish a tectonic and temporal framework for the western part of the Musgrave Block as an integral part of the NGMA mapping of this geological province.

The field and tectonic relationships between the layered basic/ultrabasic intrusions of the Giles Complex and associated country rocks, when combined with isotopic ages and thermo-barometric data, suggest a genetic model for these intrusions — the most extensive of their type on the Australian continent (Nesbitt & others, 1970: *Geological Society of South Africa Special Publication*, 1, 547–564; Daniels, 1974: *Geological Survey of Western Australia Bulletin*, 123). Earlier stud-

ies have outlined the major tectonic events (Goode, 1978: *Contributions to Mineralogy & Petrology*, 51, 137–148; Pharaoh, 1990: *BMR Record 1990/5*; Glikson & others, 1990: *BMR Research Newsletter*, 12, 18–20). Recently, two areas covering the margins of the Hinckley Gabbro — an ESE-trending ca. 40x5 km large intrusion — were mapped: the Champ de Mars area and the westernmost Hinckley Range near Charnockite Flats (Fig. 1) (Clarke, 1992: *BMR Record 92/33*). The tectonic and thermal history of the terrane is outlined below.

### Early granulites and pre-Giles Complex deformation (D1–2)

These oldest rocks comprise well-layered to massive felsic and mafic granulites of mostly supracrustal derivation, as indicated by common ortho-quartzite units and by primary layering. Evidence of two early deformation events (D1 and D2) accompanying granulite facies metamorphism is preserved (Table 1; Fig. 2). Igneous components include pre-S1 mafic granulites and post-S1 pre-S2 lenses of orthogneiss and charnockitic (orthopyroxene-bearing) granite. A penetrative S1 gneissosity is deformed by isoclinal F2 folds. Except for F2 hinges, S1 has been rotated into parallelism with S2; only rarely are isoclinal F1 folds identifiable owing to intense recrystallization during D2. Where unaffected by subsequent deformation, D2 is characterised by meso- to macroscopic, tight

to isoclinal F2 folds with E to ESE-trending axes and reclined axial planes, resulting in a shallow E-dipping S2 foliation. Whereas an S1–S2 intersection lineation is common, mesoscopic F2 folds are not associated with mineral-stretching lineation, implying deformation involving mainly pure shear. S1–2 fabrics typically comprise granoblastic interlocking mineral assemblages, in contrast to later mylonitic foliations enveloping residual S1–2 minerals.

### Giles Complex and associated granitoids

Cross-cutting contacts of the Hinckley Gabbro with the granulites indicate its emplacement has postdated S2, although gabbro-granulite contacts have mostly been disrupted by later deformation. Well-exposed intrusive contacts are also observed along the northern margin of the Kalka basic/ultrabasic intrusion and the southern margin of the Mount Davies Gabbro (Nesbitt & others, *op. cit.*). Regionally extensive K-feldspar megacrystic granite and microgranite dykes and stocks intrude banded granulites and gabbro or gabbro-derived mafic granulite of the Giles Complex. Mafic granulite and amphibolite xenoliths occur within the granitoids. Megacrystic granite stocks grade into microgranite. Charnockitic and rapakivi granites, in places grading into megacrystic granite and with inclusions of gabbro and recrystallized derivatives, occur along and in places intrude



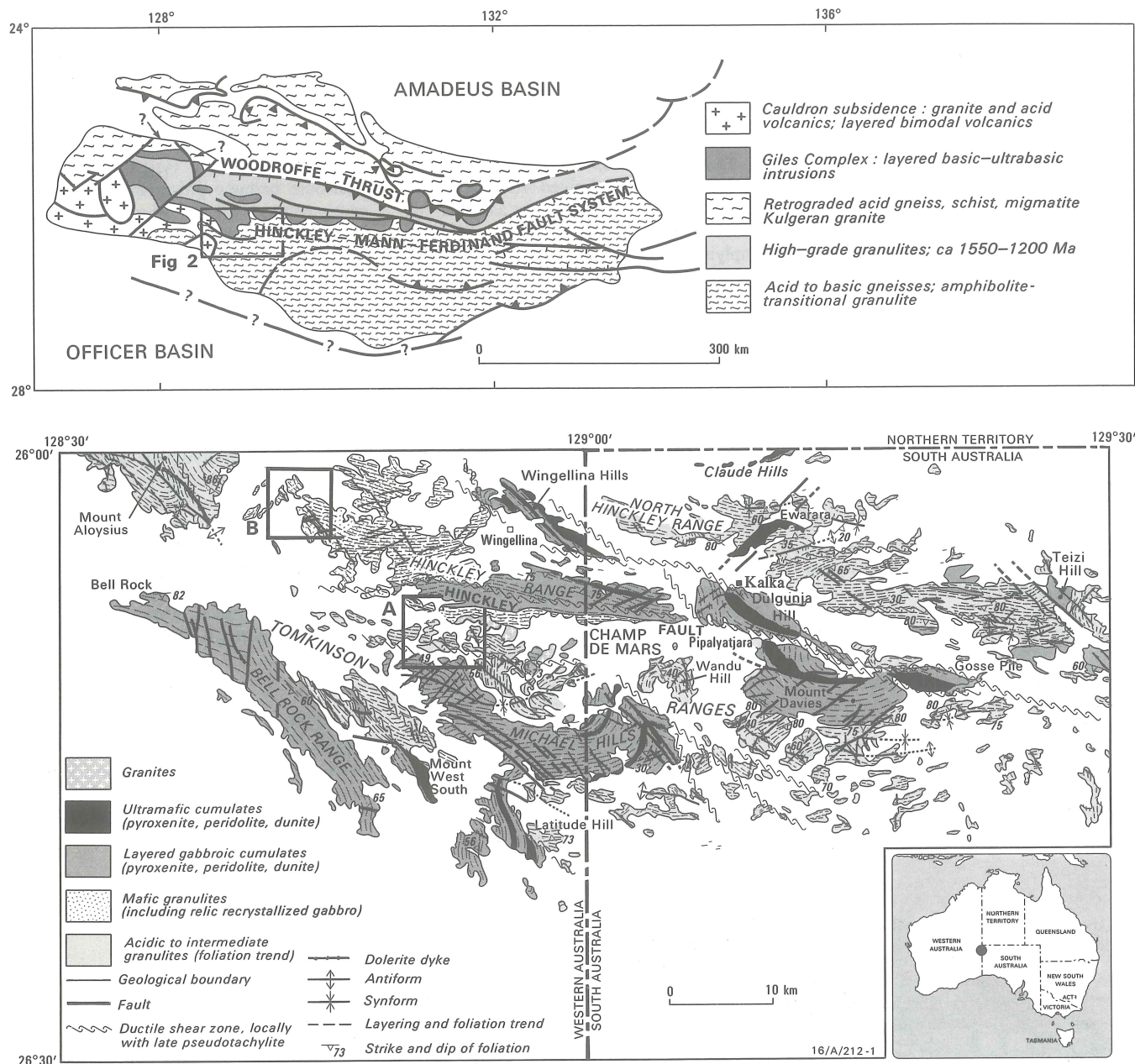


**Fig. 1. Geological sketch maps of the Musgrave Block, central Australia, and of the Tomkinson Ranges, W.A. and S.A.** The frames in the latter define the two areas reported in the present paper: A – Champ de Mars area; B – westernmost Hinckley Range–Charnockite Flats area.

the southern margin of the Hinckley Gabbro. All the above units are intruded by at least three generations of basic dykes; the oldest defined as type-A Dykes is deformed by D3 (see below). This swarm consists mostly of NW-trending and some NE and N-trending dykes.

### Post-Giles Complex deformation (D3)

D3 structures comprise upright to reclined, tight to isoclinal, mesoscopic F3 folds with amplitude and wavelength from a metre to tens of metres, with steeply dipping SE-trending S3 axial plane mylonitic foliations. In the felsic granulites, D3 resulted in widespread rotation to sub-parallelism of earlier S1–2 granoblastic assemblages to S3–L3 mylonitic fabrics. These fabrics consist of steeply plunging SW-trending L3 stretching lineations within the SE-striking steeply S-dipping S3 foliation (Fig. 2), suggesting SW-directed

compression and recrystallization under dominantly simple (rotational) shear. In general, D3 is difficult to detect in massive gabbro. However, in felsic vein-injected mafic granulites derived by recrystallization of gabbro, S3–L3 fabrics are dominant, and include penetrative rodding of felsic stringers related to simple shear rotation. Type-A dykes display marginal to complete recrystallization of primary igneous textures into granulite facies S3 assemblages; their trend results from D3 folding and is mostly aligned with the SE-trending S3 foliation. Intrusion of NW-trending type-B basic dykes, with coarse-grained plagioclase phenocrysts, cross-cut S3 foliations and thus postdate D3. Fine-grained to aphanitic, occasionally pyrite-bearing, mostly NW and NE-trending type-C basic dykes, represent the youngest intrusions.

### Mylonitic shear zones

The Hinckley Gabbro and Kalka layered intrusion are bound to the south by east-west mylonitic to ultramylonitic shear zones, referred to as the Hinckley Fault (Goode, 1978: *op. cit.*), and its off-shoots. This deformation (D4) resulted in ten to one hundred metre-wide zones of intense recrystallization, with

throws of a few metres up to about 100 m as estimated from basic dyke displacements. Southeast-directed transport is indicated by S4–L4 geometry. D4 shears are offset by N-trending D5 ultramylonite zones dipping steeply east, with D5–L5 relations indicative of SW-directed transport and apparent dextral reverse throw of a few hundred metres. Broad E-trending D6 ultramylonite zones form prominent faults, the primary example being the Champ de Mars fault (Fig. 1). The zone of pervasive D6 recrystallization is up to 500 m wide where felsic rocks are affected, or zones up to 150 m wide through gabbro; in the latter, the mylonite is imprinted by extensive pseudotachylite (Glikson & Mernagh, 1990: *BMR Journal*, 11, 509–519). The fault dips steeply south and has a steeply plunging L6 mineral-stretching lineation, suggesting its correlation with the Woodroffe thrust zone and related faults. The latter involved northward transport of the Musgrave Block over the late Proterozoic to Palaeozoic Amadeus Basin during the Cambrian Petermann Orogeny (Collerson & others, 1972: *Geological Society of Australia Journal*, 18, 379–393; Forman & Shaw, 1973: *BMR Bulletin*, 144; Glikson & others, 1990: *op. cit.*). Poorly



exposed E-trending mica-rich D7 retrograde shear zones dip north; they preserve a reverse sense of movement — for example, south of Walpa-Puka hole in the Champ de Mars area (Fig. 1).

### Tectonic and thermal evolution

The banded granulites west and south of the Hinckley Gabbro are correlated with the Mount Aloysius supracrustal layered granulites, where Rb-Sr whole-rock isochrons define ages of  $1564 \pm 12$  Ma and  $1327 \pm 7$  Ma — both interpreted as protolith ages (Gray, 1978: *Geological Society of Australia Journal*, 25, 403–414), a conclusion confirmed by preliminary U-Pb ion probe studies (S. Sun, *accompanying article*). D1 was likely associated with peak granulite facies metamorphism, dated at about 1200 Ma (Gray, 1978: *op. cit.*; Maboko & others, 1991: *Journal of Geology*, 99, 675–697). The absence of orthopyroxene-sillimanite assemblages in the granulites constrains pressures to below 70 Mpa. The basic and ultrabasic intrusions of the Giles Complex crystallized under pressures of about  $60 \pm 10$  Mpa, followed by isobaric cooling from ca.  $1200^\circ$  to ca.  $700^\circ$  (Ballhaus & Berry, 1991: *Journal of Petrology*, 32, 1–28), suggesting emplacement at lower crustal levels under granulite facies conditions, possibly similar to those during D1–2. The age of the Giles Complex is constrained to be between the ca. 1200 Ma metamorphic age of the older granulites and the ca. 1185 Ma U-Pb zircon age of intrusive porphyritic granites at Champ de Mars (S. Sun,

*accompanying article*). The isobaric cooling and the pure shear conditions suggest, respectively, that metamorphism was related to major mantle fusion event(s), which produced the Giles Complex, and to lithostatic pressures at deep (20 km) crustal levels.

Daniels (1974: *op. cit.*) regarded the granite-injected gabbro-derived mafic granulites of the western Hinckley Range as a marginal contaminated facies of the Hinckley Gabbro, implying mixing of felsic country rocks with the basic magma. However, evidence for intrusion of granitoid veins and stocks into fractured consolidated gabbro, and the common angular mafic xenoliths within the granites (Glikson & others, 1990: *op. cit.*), suggest that the felsic vein networks represent back-intrusion contemporaneous with emplacement of the Hinckley Gabbro and/or younger granitic event(s). The porphyritic and rapakivi granite stocks, pods of charnockitic granite, and numerous felsite and pegmatite veins seem broadly contemporaneous and all are affected by D3 mylonitic foliation. The onset of D3 deformation, represented by mylonitic simple shear, was probably accompanied by decompression and elevation of the terrane to mid-crustal levels (ca. 40–50 Mpa,  $>700^\circ$ ), inferred from garnet-cordierite corona textures in D3-deformed metapelitic gneisses at Cohn Hill, west of the Blackstone and Cavanagh Gabbro bodies (Clarke & Powell, 1990: *Journal of Metamorphic Petrology*, 9, 440–451).

No feeders to the Giles Complex have yet been identified, and the post-granitoid pre-D3 basic dykes (type A) clearly post-date the

Hinckley Gabbro. The younger basic dyke sets and mylonitic shear zones reflect further uplift of the terrane and recrystallization under lower grade and, in places, brittle regimes. Type B dykes may have formed feeders to volcanics of the Bentley Group (U-Pb zircon age of ca. 1060 Ma). Type C dykes which post-date metamorphism may be significantly younger. D4 and D5 mylonitic shears, involving displacements of up to a few hundred metres, contain evidence for SE-directed and SW-directed stress fields, respectively. The greenschist-to-amphibolite facies assemblages in these shear zones imply cooling between D3 and D4. The superposed latitudinal D6 faults of the Woodroffe thrust system and D7 hydrated retrograde fault zones are correlated with Cambrian northward thrusting of the Musgrave Block and with general uplift to shallow hydrated crustal levels. Young dynamic melting events are represented by pseudotachylite vein networks superposed on all the units described above, and are best manifested in dry lithologies, including gabbro and mafic dykes. These features result from shock-melting consequent on earthquakes at mesocrustal levels (Glikson & Mernagh, 1990: *op. cit.*).

For further information contact Dr G.L. Clarke (Department of Geology and Geophysics, University of Sydney), Dr I.S. Buick (University of Melbourne, Parkville), or Dr A.Y. Glikson or Dr A.J. Stewart at AGSO.

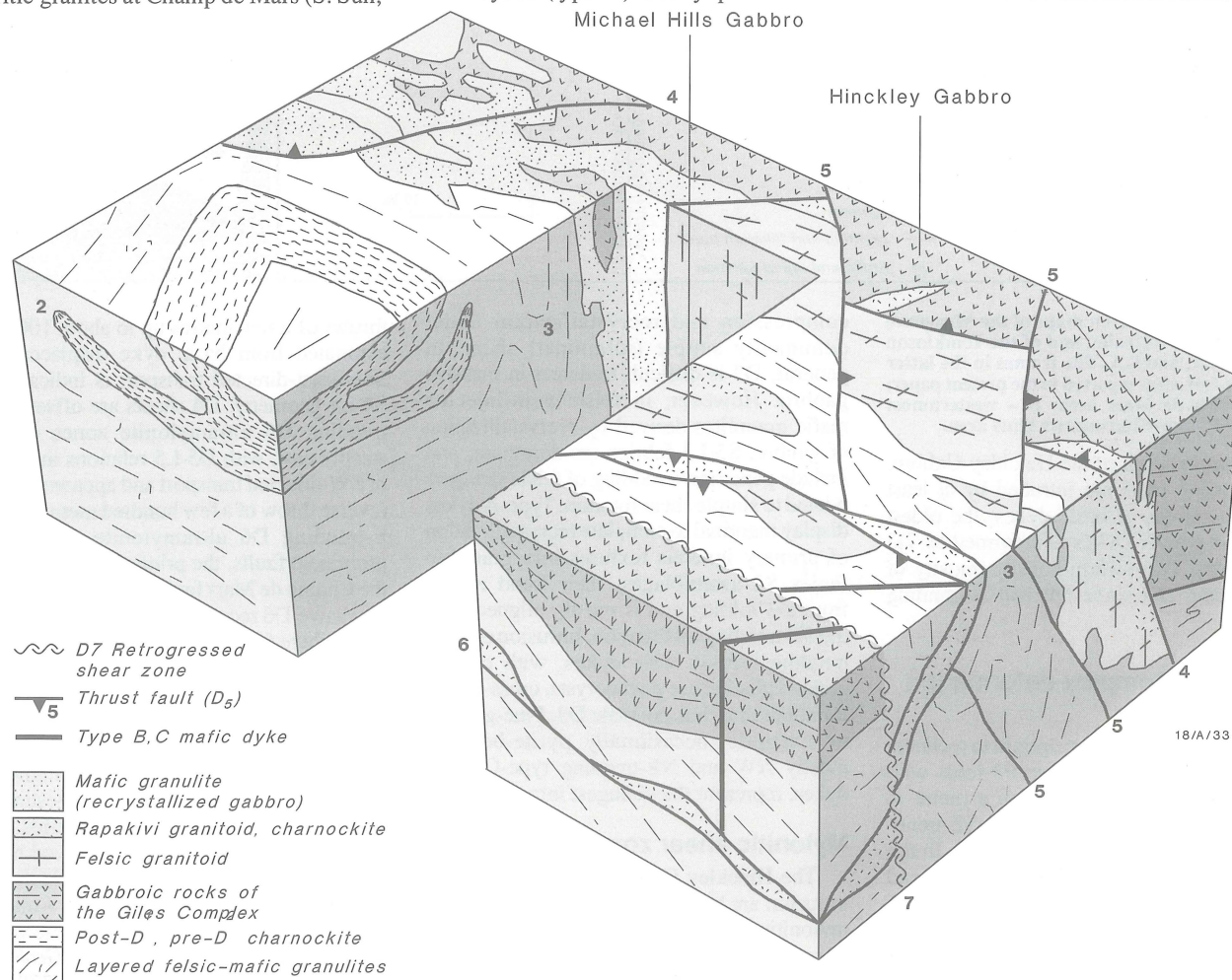


Fig. 2. A block diagram representing the relationships between the Hinckley Gabbro, layered felsic granulites, granitoid stocks, dyke systems and shear zones in the western and southern parts of the Hinckley Range, Tomkinson Ranges, W.A.



## Chinese earthquakes to rock Australian buildings

China and Australia signed a Memorandum of Understanding (MOU) in April 1990 committing Australian seismologists from AGSO and the Seismology Research Centre (SRC), and Chinese seismologists from the State Seismological Bureau (SSB), to undertake joint research into intraplate earthquakes to improve mitigation techniques and hazard assessments.

Knowledge of how strongly the ground shakes, for how long, and at what frequency, is the basic input required by structural engineers investigating the response of buildings and structures. This data is used in computer simulation and laboratory modelling of the effects of the earthquake on structures, so that better building codes and structural design rules can be developed. Civil engineering departments at Melbourne and Adelaide Universities have large computer-controlled shaking tables on which they have modelled structures using a AGSO strong-motion record of a Tennant Creek aftershock.

One of the two joint programs involved coupling two SRC designed and manufactured digital recorders (Kelunji) to SSB accelerometers and installing the accelerographs near Tangshan, China. One of these was set up by Peter Gregson (AGSO) and Gary Gibson (SRC) during their visit in October/November 1991; the other by SSB seismologists a few months later. Tangshan was destroyed by a magnitude 7.6 earthquake in July 1976 and some 250 000 people are reported to have died. No measurement of the near-field ground motion was obtained.

In contrast to Australia, earthquakes occur more frequently in China and the period of recorded Chinese history is more than ten times longer. The tectonic setting (intraplate) and earthquake mechanisms in parts of China are similar. It is hoped that important recordings of the near-field ground motion can be obtained more rapidly in China than Australia, and used in both shaking table experiments and revision of the Australian building code.

Recent earthquakes near Tangshan triggered the two Kelunji recorders, producing about thirty accelerograms. The largest of them, in February 1992, had a magnitude 4.4, and was less than 20 km from the recorder where the peak accelerations was about 0.03 g. In contrast to accelerograms recorded in Australia from similar-sized events at comparable distances, the Chinese records seem to have lower amplitudes, longer duration and lower frequencies. Detailed analysis must await receipt of the digital data.

For further information contact Kevin McCue, Australian Seismological Centre, AGSO.

## Zircon U/Pb chronology, tectono-thermal and crust-forming events in the Tomkinson Ranges, Musgrave Block, Central Australia

The Musgrave Block is an important geological feature between the Proterozoic Arunta and Gawler Blocks, and the Paterson and Albany–Fraser belts. The dominant event in its evolution may be correlated with the global Grenville Orogeny (Fig. 1). Geochemical analysis and SHRIMP U/Pb zircon dating of major rock units in the Tomkinson Ranges were carried out as part of the NGMA Musgrave Project. This study aims to define major tectono-thermal and magmatic events; to correlate between various rock types and units; and to define the age and genetic relationships between the layered mafic/ultramafic Giles Complex, regional granulite-facies metamorphism and widespread porphyritic and rapakivi granites. Finally, the geological relationships between the Musgrave Block and neighbouring blocks and the possible connection with the global Grenville Orogenic event are explored.

Clarke & others discuss the intrusion, deformation and recrystallisation history of the Giles Complex and host granulites (see their article in *present issue* for regional geology and geochronological events).

The present article is concerned with the following questions:

- What are the differences in age and style of crust formation between the Musgrave and its neighbouring blocks?
- Was the thermal pulse associated with the Giles Complex also responsible for the regional granulite-facies metamorphism?
- Is the rapakivi granite intruding the Hinckley Intrusion the result of mixing of porphyritic granite and mafic rock?
- What are the genetic relationships between different generations of mafic dykes and the Giles Complex, on one hand, and younger mafic and felsic igneous rocks, on the other?
- How widespread in the Musgrave Block are felsic volcanics and granites with chemistry similar to the Tollu Volcanics, which are highly enriched in K, Rb, Ba, Th, U, Nb, Zr, Y, and rare earth elements (e.g. La, Ce, Nd)? How were these A-type granites and volcanics generated?

### SHRIMP U-Pb zircon ages

New zircon ages, using the SHRIMP at the Research School of Earth Sciences, ANU, confirm earlier studies using whole-rock Rb-Sr dating (e.g. Gray, 1978: *Journal of the Geological Society of Australia*, 25, 403–414). The ages of various events, mainly

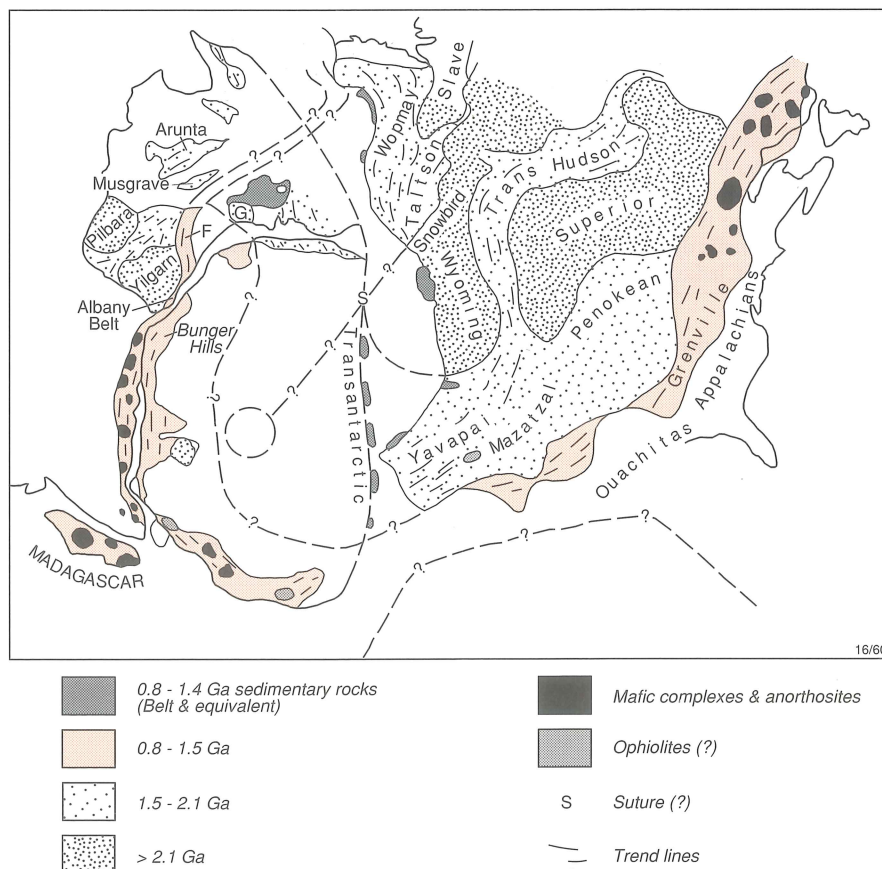


Fig. 1. Cartoon with generalised Precambrian features of part of Gondwana and North America, and their possible correlation. F for Fraser belt; G for Gawler craton. Modified and published with permission after Figure 3 of Moores (1991: *Geology* 19, 425–428).



based on whole-rock Rb-Sr dating, are summarised in Table 1 of Clarke & others (*this issue*). SHRIMP U-Pb zircon dating provides more accurate ages, in favourable circumstances, and can distinguish multiple thermal events. For example, zircons from felsic granulite between Michael Hills and Mt Davies (sample 69-1304 from location 20 of Gray, 1978) give a near-concordant age of  $1305 \pm 8$  Ma (Rb-Sr age  $1358 \pm 40$  Ma) for the possibly volcanic protolith, whereas metamorphic overgrowths of zircon are  $1223 \pm 7$  Ma old. The Minno Granite from location 7 of Gray (1978), south of the Kalka Intrusion was emplaced before D2 deformation, and well-zoned, slender igneous zircons give a concordant age of  $1198 \pm 6$  Ma (Rb-Sr age  $1204 \pm 17$  Ma). Inherited zircon cores indicate an age of  $1296 \pm 10$  Ma for the source rock (Fig. 2). Zircons from a banded felsic granulite from Mount Aloysius suggest a protolith age of about 1530 Ma and granulite-facies metamorphic age of about 1200 Ma. In addition, two age groupings of about 1300 Ma and about 1400 Ma are tentatively identified and may correspond to other metamorphic events.

A porphyritic granite, post-dating the Giles Complex from Champs de Mars (Fig. 1 in Clarke & others, *this issue*), contains abundant igneous zircons which define an age of  $1185 \pm 5$  Ma. The emplacement age of the Giles Complex can thus be constrained to between granite intrusion at 1185 Ma and granulite facies metamorphism at 1200 Ma. To clarify the relationship between the Giles Complex and the granulite-facies metamorphism, one future approach will be to date features formed directly by the Giles Complex, such as 'back intruded' felsic dykes and contact metamorphic rocks.

Zircon U/Pb dating of the Tollu Volcanics (related to the cauldron subsidence) of the Bentley Group (west of the area shown in Figure 1 of Clarke & others, *this issue*) and a 'granophyre' sample from the Bell Rock Intrusion have both a similar chemical composition as well as a similar age of about 1060 Ma. This age is within the age uncertainty of Type B mafic dykes of the Musgrave Block (Table 1 of Clarke & others, *this issue*).

## Nd isotope model ages and crustal residence times

Sm-Nd model ages ( $T_{DM}$ ) of six samples (1770–1890 Ma) reported by McCulloch (*Geodynamic Series* 17, AGU, 115–130, 1987; see also for definition of the depleted mantle model age,  $T_{DM}$ ) indicate that the protoliths of the Musgrave Block had a younger crustal residence time (approximately an average age for source rocks last separated from the mantle) than the Arunta Block (three analyses, 2120–2190 Ma). Additional new data from both Blocks confirm this earlier conclusion. Our extensive sampling coverage in the Tomkinson Range give a broader range of Nd  $T_{DM}$  model ages (1460–1910 Ma). The young model ages of 1460–1570 Ma are represented by the Tollu Volcanics, a 'granophyre' within the Bell Rock Intrusion (with a zircon age of about 1060 Ma) and related granites. Felsic granulites of possible volcanic origin from Mount Aloysius (protolith age ~1550 Ma) also have young  $T_{DM}$  model ages of 1620–1740 Ma. This suggests new crustal formation at ~1550 Ma with only minor contribution from older sources, as opposed to melting of older basement rocks. Metasediments from Mount Aloysius have  $T_{DM}$  model ages ranging from 1610 Ma (meta-arkose of local origin) to 1900 Ma (sillimanite gneiss). Felsic granulites with protolith ages of about 1300 Ma from several locations south of the Hinckley Fault (Fig. 1 in Clarke & others, *this issue*) have  $T_{DM}$  model ages of 1660–1780 Ma, similar to model ages for ~1550 Ma Mount Aloysius granulites. Granites generated during the 1200 Ma granulite-facies metamorphism at Mount Aloysius, Ewarara and Minno (south of the Kalka Intrusion) have Nd  $T_{DM}$  model ages of 1680–1860 Ma, similar to those of the country rocks.

Nd  $T_{DM}$  model ages of porphyritic and rapakivi granites in the Champs de Mars area are of special interest for testing models of magma mixing. Two samples of porphyritic granite, having  $T_{DM}$  model ages of 1877 and 1905 Ma, are among the oldest in the Tomkinson Range, with low initial  $\epsilon_{Nd}$  values of -3.7 and -4.2 at 1185 Ma emplacement time, whereas four samples of rapakivi granite have

considerably younger model ages of 1675–1787 Ma and higher initial  $\epsilon_{Nd}$  values of -1.4 to -3.1. In addition to the possibility that rapakivi granites had an origin independent of porphyritic granites, these data may be interpreted either in terms of mixing between a porphyritic granite magma and an evolved mafic magma, or partial melting of a mafic source with a young model age and a higher initial  $\epsilon_{Nd}$  value. Both interpretations are consistent with the rapakivi granites being associated with and intruding the Hinckley mafic/ultramafic Intrusion, and being generally more mafic (consistent with assimilation) than the porphyritic granites.

## Giles Complex and mafic dykes

Ballhaus & Glikson discussed in the April 1992 issue of *BMR Research Newsletter* the magmatic-metamorphic evolution and economic potential of the Giles Complex. They suggested that individual intrusive bodies had similar tholeiitic parent magmas in the mantle, but experienced different polybaric fractionation paths. On the basis of the chemistry of some 'chilled' samples and potential feeder dykes, as well as model calculations using cumulate rocks, the parent magma composition with an MgO content of 12% (see Table 1) was estimated. It is characterised by low  $TiO_2$  ~0.8%,  $P_2O_5$  ~0.09%, La ~7 ppm, Nb ~3 ppm, Sr ~200 ppm, and Zr ~70 ppm - indicating magma generation by a large degree of mantle melting at shallow depths (30–50 km?). The less abundant contemporary, or slightly younger mafic dykes have higher contents of these elements (e.g. 1.6%  $TiO_2$ , 150 ppm Zr), indicating that they were generated by smaller degrees of melting. Sr and Nd isotopic analyses of samples from Kalka and Wingellina Intrusions show considerable variation of initial  $^{87}Sr/^{86}Sr$  (0.704 to 0.708) and  $\epsilon_{Nd}$  values (+2 to -2), suggesting different extents of crustal assimilation by the magma. The estimated parent magma composition of the Giles Complex and contemporary mafic dykes are similar to basalts generated in many modern continental rifts.

Chemical similarity of ~1060 Ma metamorphosed, NW-trending Type B mafic dykes (Table 1 of Clarke & others, *this issue*), and the Mummawarrawarra Basalt of the Bentley Group (Table 1) suggests that they may be genetically related.

## Rock chemistry: implications for tectonic environment and melting

Chemical data (Table 1) and Nd isotope model ages, discussed earlier, place constraints on the tectonic environment and conditions of melting. Compositions of basalts and mafic dykes (Table 1) of various ages from the Tomkinson Range are consistent with an origin in an intraplate environment rather than a convergent margin. Nd isotope model ages of the source rocks of about 1300 Ma felsic protoliths and 1200 Ma granites are similar to those of 1550 Ma sedimentary and igneous protoliths of the felsic granulites. Thus, these 1300 and 1200 Ma rocks could simply have been derived by remelting of ~1550 Ma crust.

Chemical compositions of the 1185 Ma porphyritic granites and the 1060 Ma Tollu

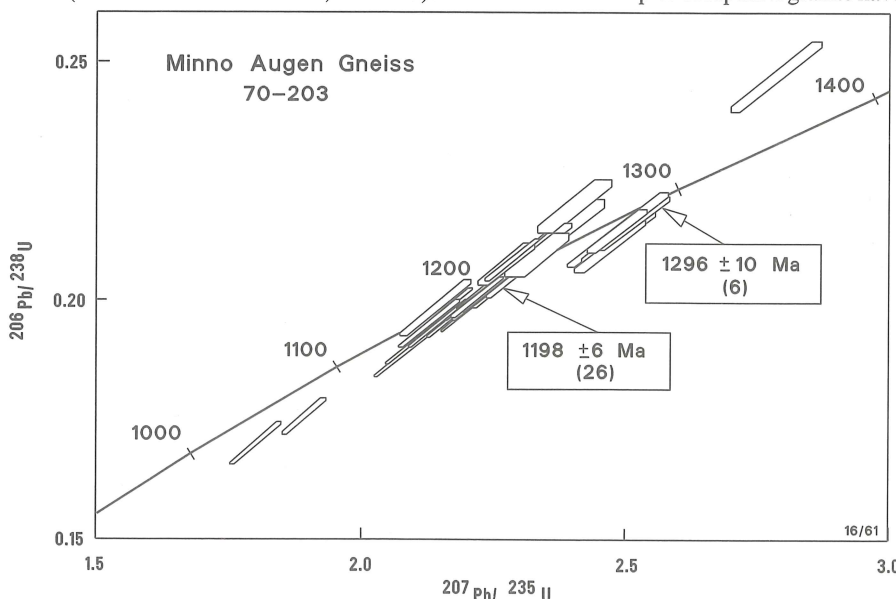


Fig. 2. Concordia diagram for zircons from Minno granite gneiss, emplaced during granulite facies metamorphism.  $1198 \pm 6$  Ma is the time of granite emplacement whereas  $1296 \pm 10$  Ma the age of the protolith.



Table 1. Chemical composition of representative meta-igneous rocks and mafic dykes, Tomkinson Range area (major elements-weight %; trace elements-ppm)

	1550 Ma Mount Aloysius		Estimated Giles Parental magma	1185 Ma granites Champs de Mars		~1060 Ma Bentley Group			~800 Ma mafic dyke
	mafic Volc.	felsic Volc.		por-phyrritic	rapakivi	mafic dyke	Mumawa- rrowarra	Tollu Volc.	
SiO <sub>2</sub>	47	73	49	68	65	51	51	72	50
TiO <sub>2</sub>	1.5	0.2	0.8	0.5	1.3	0.9	1.3	0.4	1.7
Al <sub>2</sub> O <sub>3</sub>	15.5	15.3	14	14.5	13.1	16	13.5	12.5	14.7
ΣFeO	13.0	1.0	11	3.4	6.3	11	11	3.2	12.0
MnO	0.18	0.02	0.17	0.06	0.11	0.16	0.15	0.09	0.17
MgO	8.0	0.3	12	0.7	1.2	6.7	6.8	0.1	6.5
CaO	11.4	1.8	11	2.0	2.9	~10	~10	1.5	11
Na <sub>2</sub> O	(1.2)	4.7	1.6	3.4	2.7	2.4	2.3	3.6	2.2
K <sub>2</sub> O	(0.7)	3.6	0.3	5.1	4.6	0.7	1.3	5.5	0.3
P <sub>2</sub> O <sub>5</sub>	0.13	0.03	0.09	0.08	0.6	0.16	0.18	0.03	0.16
Zr	77	110	70	470	560	120	150	950	105
Nb	4	2	3	27	32	5	6	80	5
Y	32	5	18	140	90	26	29	180	27
La	11	19	7						10
Ce	20	32	17	(280)	(200)	(25)	(30)	(280)	26
Nd	14	9	10	140	100	14	18	140	18
Th	—	4	—	100	30	—	—	45	—
U	—	0.5	—	8	2	—	—	6	—
Ga	21	23	13	21	21	18	18	35	16

Volcanics, as well as related granophyres and granites, show affinities to A-type granites, with high Zr, Nb, Y, REE, Th, U contents, in addition to high Ga/Al ratios. However, they have quite different Nd model ages and characteristic element ratios. Porphyritic granites in the Champs de Mars area have the oldest Nd isotope model ages of the samples analysed, consistent with an origin by melting of refractory crust after granulite facies metamorphism (1200 Ma). The generation of these porphyritic granites may have been caused by the thermal anomaly associated with the Giles Complex, if one assumes a similar age. The Tollu Volcanics, in contrast, have considerably younger Nd isotope model ages (1460–1570 Ma) and thus cannot have been derived from pre-existing felsic crust. They have very high Nb and Th contents (up to 100 ppm) and Nb/Y and Nb/Ce ratios, features that are characteristic of differentiates of intraplate basalt (e.g. Eby, 1992: *Geology*, 20, 641–644), and positive initial εNd values similar to con-

porary basalts of the Bentley Group. The Tollu Volcanics were, therefore, probably derived through extensive fractionation of basaltic magma in stable intraplate magma chambers.

### Broader tectonic implications

Crust-forming episodes at 1550 and 1300 Ma, observed in the Musgrave Block, have no counterparts in the neighbouring early Proterozoic Arunta and Gawler Blocks, suggesting an independent geological evolution (Shaw & Black, 1991: *Australian Journal of Earth Sciences*, 38, 307–332). On the other hand, 1300 and 1200 Ma magmatic and metamorphic events are well documented in the Albany-Fraser Province (Fig. 1) to the southwest of the Musgrave Block (e.g. Black & others, in press: *Precambrian Research*). A connection to the same tectono-thermal events experienced in Albany-Fraser belts can be suggested. Moores (1991: *Geology*,

19, 425–428) recently proposed that the Albany-Fraser Province was part of a Grenvillian fold belt (1300–1100 Ma), which extended from the Appalachian and Antarctica, into the Albany-Fraser Province (Fig. 1). Moores postulated that this Grenvillian belt extended farther to the south of the exposed Musgrave Block (Fig. 1). This would explain the apparently contrasting tectonic environments of the Musgrave Block (intraplate) and Albany-Fraser province (collision) even though both are of the same age, i.e. 1200 Ma. This proposal, however, needs closer examination. Available geological and geophysical (gravity and magnetic) data from central and western Australia require a more complicated Grenvillian tectonic evolution than shown in Figure 1. Additional research is required.

For further information, contact Dr. Shen-su Sun or Dr. John Sheraton (Minerals and Land Use Program) at AGSO.

## Aquifers at risk: towards a national groundwater quality perspective

The Australian National University's Centre for Continuing Education is sponsoring a conference in Canberra, 15–17 February 1993, in co-operation with the Australian Geological Survey Organization (formerly B.M.R.), to provide a scientific and community forum on a range of groundwater quality issues. This conference will be the ninth in the series of *Issues in Water Management*.

High-salinity groundwaters have always been a constraint on water supply development in Australia. Where groundwaters contain high concentrations of naturally occurring substances, such as nitrate, fluoride, and heavy

metals, consumption of these groundwaters may constitute a significant health hazard.

Numerous questions arise: Where are the major occurrences of these substances and what can be done for remediation of small-scale, local water supplies? In regard to several important inland and aquifers undergoing increasing salinity due to excessive withdrawal of groundwater, how best can these systems be managed in the face of increasing water consumption and potential sealevel rise caused by global warming?

Several important *regional* groundwater systems are known to be polluted by sewage and agrichemicals. Some aquifers are used for

domestic purposes, whereas others infiltrate sensitive surface waters. What modifications are needed in waste management, land use, and agricultural practice to control this pollution of both subsurface and surface waters? Furthermore, an increasing number of *local* aquifers are polluted by toxic chemical and other wastes, and petroleum products. How can these problems be managed: can polluted aquifers and land be effectively rehabilitated? Do we have adequate health and environmental protection standards?

The processes involved in groundwater quality deterioration, and the management, remediation and protection of the nation's



groundwater systems, will be reviewed in the above-mentioned conference.

Contributions are invited, which can be in the form of poster displays or workshop

sessions. Abstracts will be considered by the conference committee and should be forwarded to Shirley Kral, Centre for Continuing Education, Australian National University,

GPO Box 4, Canberra, 2601.

For further information, please contact Shirley Kral, telephone (06) 249 4580, and fax (06) 257 3421.

## Salt lake dynamics, wastewater disposal, and evaporation basins

New insights into salt lake dynamics have been obtained by AGSO (formerly BMR) researchers in the Murray Basin, southeast Australia, which have considerable implications for wastewater disposal. The Murray Basin is an important agricultural region that suffers a serious problem of land and water salinisation caused by rising water tables. The control of rising saline water tables and protection of the Murray River necessitates pumping and disposal of saline wastewater. Natural salt lakes are favoured sites for disposal, as it is possible to use the natural process of evaporative concentration. However, the environmental impact of the resultant concentrated brines on the underlying groundwater system is of concern, and predictive modelling is needed. This forms the rationale for a research project on groundwater discharge and salt lake dynamics undertaken by AGSO in collaboration with CSIRO, and sponsored by the Murray-Darling Basin Commission under its Natural Resources Management Strategy.

Salt lakes in the Mallee region, Murray Basin, are the locus of groundwater dis-

charge from a widespread regional aquifer, the Parilla Sand. Groundwater in this aquifer has a salinity close to seawater, i.e. about 35 g/L total dissolved solids. In the groundwater discharge zones, however, brine has developed by evaporative concentration, with a salinity of up to 350 g/L, nearly ten times the salinity of seawater. Following a reconnaissance of discharge zones, sites at Nulla, Scotia and Mourquong were selected for detailed field investigation (Fig. 1). Each of these groundwater discharge zones exhibits a characteristic suite of landforms, including salt lakes, gypsum flats and lunettes (crescentic dunes). Many of these features are of Late Pleistocene age, and there is evidence of several periods of lacustrine deposition in periods of wetter climate.

Special technology has been developed for salt-lake drilling by AGSO technical staff. This has enabled coring to a depth of 12 m despite soft, wet surface conditions. A tripod-mounted drilling rig is assembled on site using a hovercraft to transport the components on the salt lake. Porewaters are extracted from the drill cores in a field laboratory, so that salinity profiles can be determined on site.

The Nulla Spring Lake is underlain by 5 m

of clay, and beneath that by the Parilla Sand. Drilling has established that salt generated at the surface diffuses through the clay and enhances the salinity of the top of the aquifer. At the bottom of the aquifer, higher salinities are due to the settling of fossil brine generated by a larger Nulla lake in a wetter period of the late Quaternary (Fig. 2). The advective settling of brine requires higher vertical permeability, and probably took place before the deposition of the clay layer. Under present-day conditions, the clay seal restricts the ability of the lake to draw down the water table in the surrounding country, suggesting that salt lakes — like Nulla Spring Lake — may be effective as sites of enhanced discharge schemes aimed at lowering regional water tables to relieve land salinisation. For this to be feasible, the discharge rate would have to be increased artificially. However, clay-bottomed lakes — such as Nulla Spring Lake — are ideal for the retention and evaporation of waste waters.

At Scotia, a sand-floored salt lake was studied. Drilling established that the Parilla Sand is about 8 m thick beneath the salt lake and overlies the mid-Tertiary Geera Clay, which is an effective aquitard. A brine pool

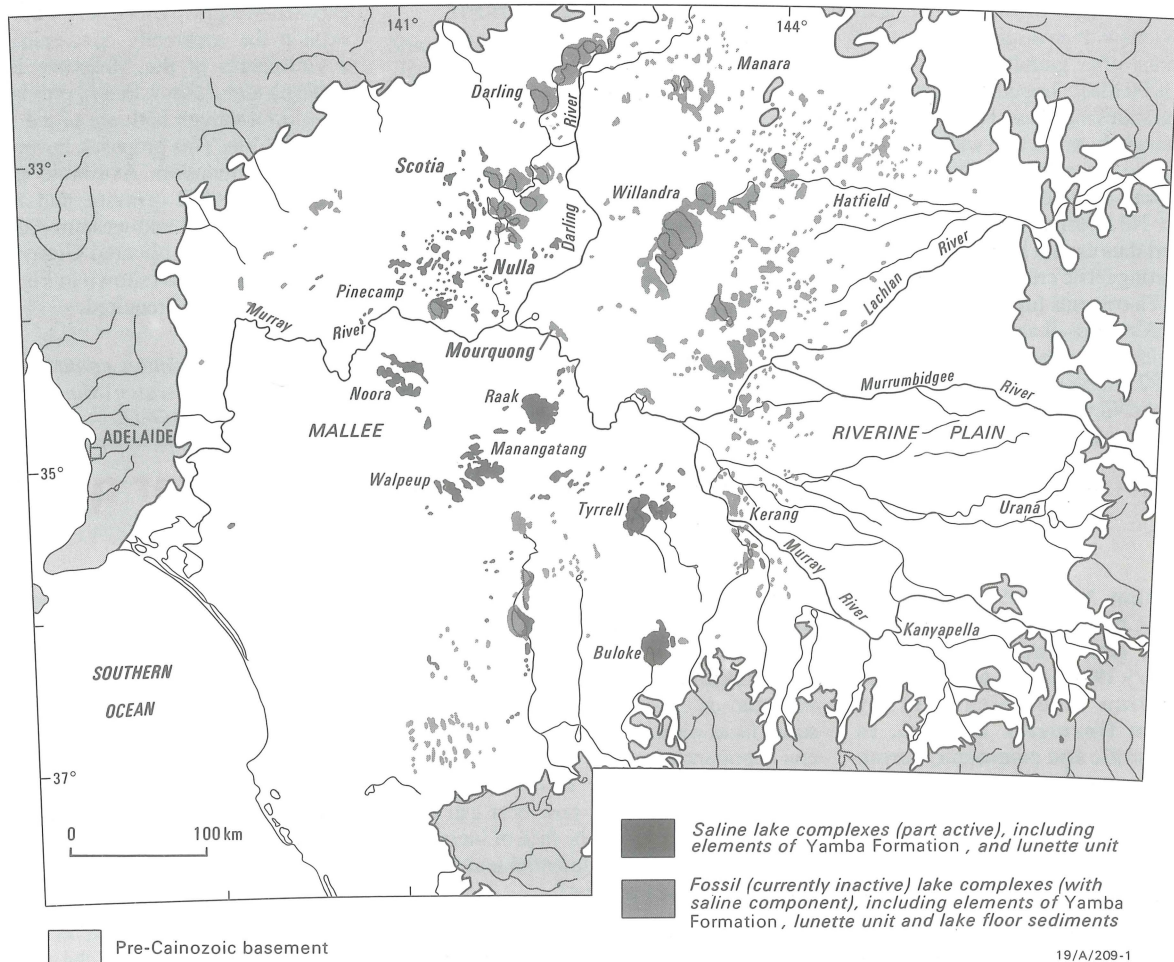


Fig. 1. Location map showing groundwater discharge zones in the Murray Basin and the locations of investigated sites.



has developed in the sand and spread laterally, but its downwards movement has been impeded by the clay. There is evidence of relatively minor enhancement of salinity in the lower aquifer beneath the clay.

The Mourquong site is an operating evaporation basin. At nearby Buronga, a saline groundwater interception scheme protects the Murray River. Saline groundwater is pumped from the Parilla Sand aquifer, transported by pipeline and disposed of in the Mourquong Basin — a former groundwater discharge complex. About 4 m of relatively thinly bedded gypsiferous sands and clays overlie several metres of clay and the Parilla Sand at this site. Drilling has shown that evaporated brine fills the gypsiferous sands and clays, but its downwards movement is retarded by the underlying lacustrine clay. The brine has lower salinity in the southern part of the discharge zone, which is closer to the site of wastewater discharge.

Modelling by CSIRO collaborators has indicated a likely mechanism for downwards brine movement by the process of salt “finger” detachment after a critical point of salt layer instability is reached. This critical point is partly a function of the vertical permeability of the sediments, with rapid advection favoured, rather than slow diffusion, when the permeability is high. It is also a function of the evaporative flux at the site. Thus, the development of brine pools should occur preferentially beneath brine pools in sand-bottomed salt lakes, now and in the past. However, the presence of at least thin clay layers appears to be necessary to allow time for the evaporation process to proceed.

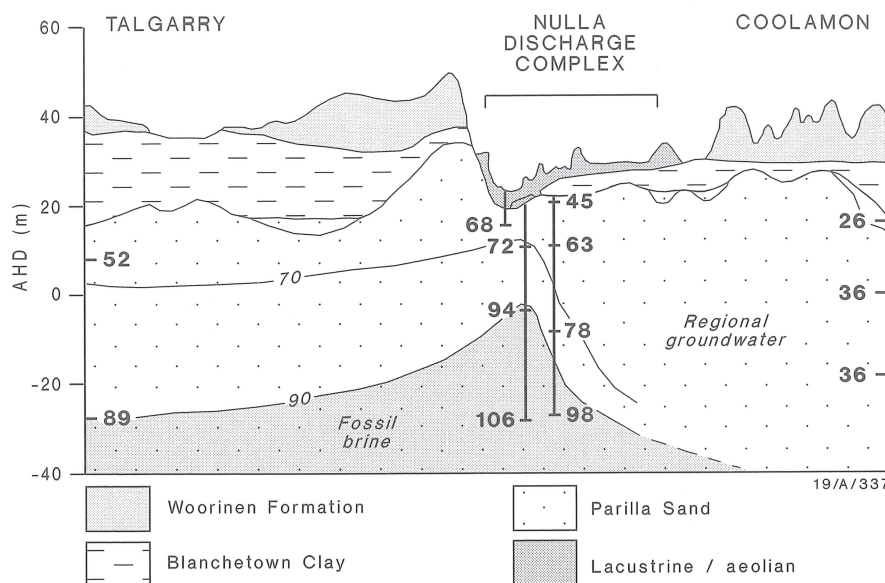


Fig. 2. Salinity (g/L) of groundwaters in the regional Parilla Sand aquifer beneath the southern area of the Nulla Discharge Complex. Regional groundwater has a salinity of about 35 g/L, brines in a present-day lake (Nulla Spring Lake) reach 340 g/L, and fossil brines beneath the Discharge Complex are typically 100 g/L.

Field data is now being evaluated and a report for the sponsoring agency is being prepared. With about 90 operating evaporation basins presently in the Murray Basin, and more proposed, the results of this work will have considerable application. Increasingly, natural salt lakes used as evaporation basins will be required to lock up large amounts of salt for long periods of time, and the environmental impact of this stored salt will have to be minimised. The salinisation of natural wet-

lands in lake basins is an associated issue that is emerging in the Murray Basin. This has occurred in several localities owing to the displacement of saline groundwater by irrigation-induced groundwater mounds or river control works.

For further information, contact Gerry Jacobson or Jim Ferguson at the AGSO (Environmental Geology and Groundwater group).

## New mapping in the Bathurst Sheet area — increased metallogenic potential

The Lachlan-Kanmantoo Fold Belts Mapping Accord Project is a six year collaborative program by AGSO, NSW Department of Mineral Resources, Geological Survey of Victoria, and South Australian Department of Minerals and Energy to provide a new generation of digital geological data on the Kanmantoo — and especially the Lachlan Fold Belt — supported by tectonic, metallogenic and geomorphic/regolith interpretations based on the new data. AGSO's field mapping has been completed on the Blayney and Oberon 1:100 000 sheet areas; digital editions of the maps using Arc/Info will be available in early 1993. Interpretation of the detailed geophysical survey, flown by Geoterrex at 250 m line spacing, has greatly assisted the mapping program, and preliminary digital magnetic and radiometric interpretation maps have been prepared.

### Epithermal and porphyry-style mineral potential

The field mapping has considerably increased the geological understanding and upgraded the metallogenic potential. In the Blayney sheet area, zones of potential Cu/Au mineralisation are indicated in buried Ordovi-

cian shoshonitic subvolcanic intrusive complexes. One complex, centred 15 km west of Blayney, and associated with the coeval Forest Reefs Volcanics, consists of a semicircular belt of monzonitic and syenitic intrusives which define a central cauldron subsidence zone about 6 km across (Fig. 1). Subsidence of the central basinal structure indicates that the whole area is underlain by a large intrusion, and that the overlying basaltic breccias, volcanoclastics, and more fractionated trachytic volcanics, have collapsed into the underlying magma chamber. At the northern rim of the structure, the volcanics have undergone intense hydrothermal alteration, producing abundant propylitic alteration and pyrite development. Original magnetite in the volcanics was destroyed by the hydrothermal system and the alteration zone is well displayed on the aeromagnetic image. Associated with this system are scattered veins and plugs of quartz-tourmaline-clinozoisite-sulphide rock which we interpret as distal products of the hydrothermal system. We suggest that the main zone of alteration is still buried, perhaps at the interface between the underlying intrusion and the roof-rocks.

This system has many analogies in the shoshonitic Lihir Island caldera (Wallace & others, BMR Report 243, 1983) which hosts the Ladolam gold deposit (reserves of 42 mil-

lion ounces, or 1200 tonnes — PNG Resources, July–December 1992). The Forest Reefs caldera is about twice the diameter of the Lihir Island caldera. Our chemical analyses of relatively unaltered volcanic rocks at Forest Reefs indicate a high gold content around 5 ppb, and sulphur undersaturation at magmatic temperatures. Thus, gold would concentrate in the magma during fractionation, and would be strongly partitioned into an evolving hydrothermal fluid phase. Assuming a magma body of 10 km diameter and 2 km thick with 5 ppb gold at Forest Reefs, some 80 million ounces of gold are potentially available for partitioning into the fluid phase. Climax Mining has reported several small near-surface gold deposits in exploration over the past 4 years (Climax Mining Annual Reports 1988 to 1991), but deeper exploration has not yet been carried out.

The geophysical survey has revealed detailed zonation and structures within Ordovician and Carboniferous plutons. Although subdivision of some of the bodies had been mapped previously, poor exposure has generally limited traditional surface geological investigations. Utilising the airborne data and surface magnetic susceptibility and radiometric measurements, geological mapping has confirmed regular concentric zonation of



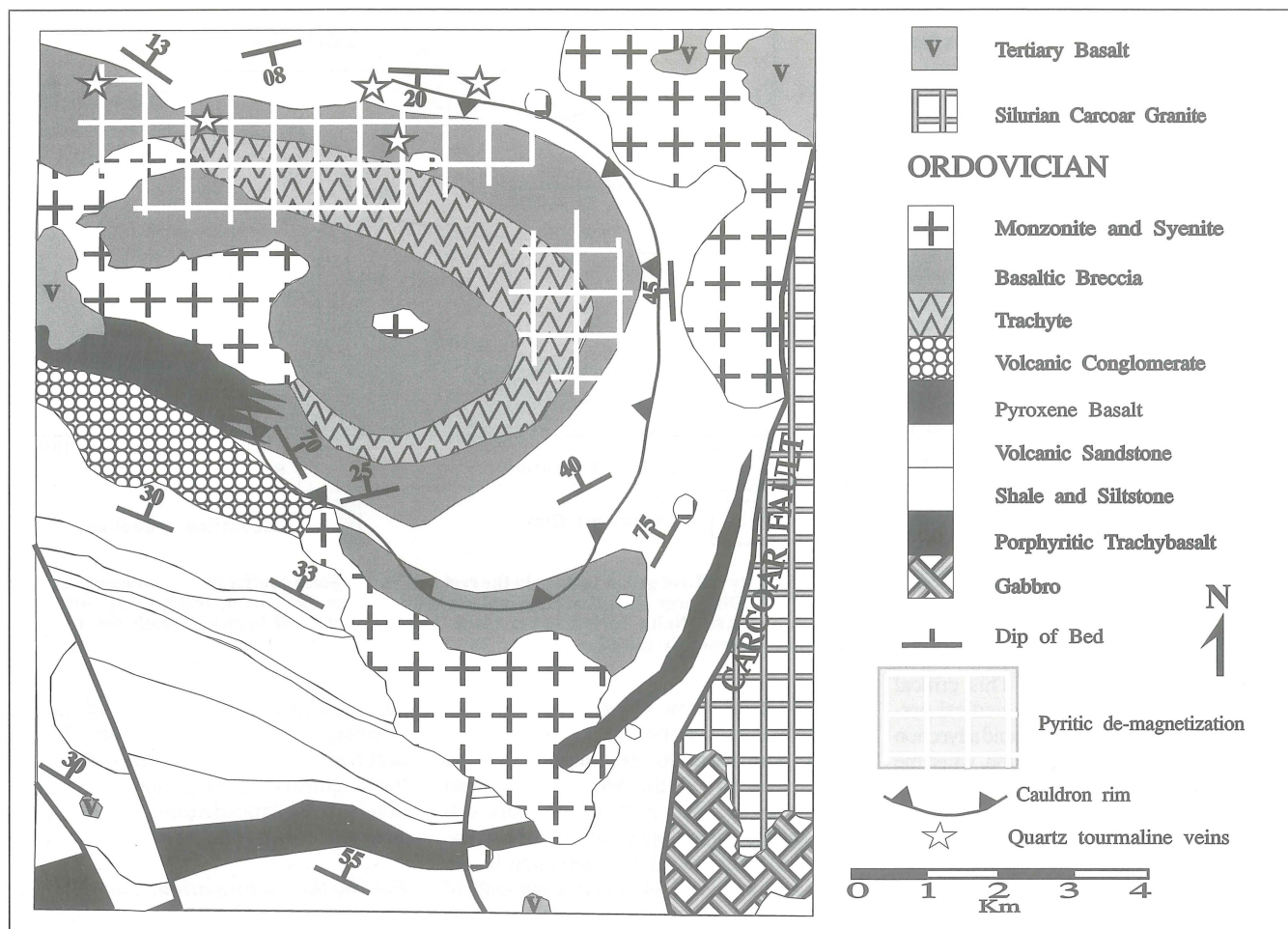


Fig. 1. Forest Reefs Volcanics cauldron subsidence zone.

granites of the Tarana, Oberon and Bathurst plutons, and monzonites of the Prince of Wales and Moorilda plutons. Magnetic lows within the centre of some of these plutons may indicate more highly fractionated phases and/or alteration, and potentially favourable sites for gold and base-metal mineralisation.

### Metamorphic gold potential

In the Oberon sheet area, the new mapping has defined a considerably larger area of the potentially gold-bearing Ordovician Rockley Volcanics than previously mapped. The volcanics conformably overlie, and are interbedded with quartz-rich turbidites and black mudstones. They have now been found to extend south around the Native Dog syncline, almost to the southern margin of the Oberon 1:100 000 sheet area. They also extend north into the Mount Diamond embayment of the Tarana Granite; an area previously mapped as Silurian sediments. In addition to the ultramafic members of the Rockley Volcanics known from near Dog Rocks, a further belt of ultramafic rocks has been discovered at Dunns Plains to the west of Rockley.

We have analysed for gold down to the 1 ppb level on all our geochemical samples of Ordovician igneous rocks. The primary high (5 ppb) gold content of low metamorphic

grade Ordovician volcanic samples is replaced by low levels at higher grades (<1 ppb at amphibolite grade). Every 1 ppb removal of gold per cubic kilometre of rock liberates 100000 oz gold into metamorphic fluids. Gold deposits, such as Lucky Draw, Browns Creek, Gallimont, Caloola and Gilmandyke, which occur in contrasting rocks immediately adjacent to Ordovician volcanics, may have formed when metamorphic fluids reacted with these rocks as they escaped the Ordovician volcanic pile. The newly mapped boundaries of the Rockley Volcanics are potentially new exploration targets.

### Submarine volcanic massive sulphide potential

The Silurian stratigraphy of the Hill End Trough sequence can be correlated across both 1:100 000 sheet areas, but formalizing of nomenclature must await correlation with sequences being mapped by the NSW Geological Survey to the north of the Bathurst Batholith. Submarine felsic volcanics occur at the base in most areas. These are overlain by a dominantly fine-grained clastic sequence, which is in turn overlain by a sandy and volcanoclastic facies. In places, the volcanoclastic facies is replaced by mafic volcanics towards the bottom, and intermediate to felsic

volcanics towards the top. The highest parts of the sequence are in the Trunkley area, where the volcanoclastic unit is overlain by another fine-grained sequence, informally known as the Trunkley slate. The distribution of primary felsic submarine volcanics has now been delineated and can be used as a basis for submarine volcanic exhalative massive sulphide exploration.

The high gold content of Ordovician volcanics, which unconformably underlie the Silurian sequences with massive sulphide potential mentioned above, also gives an added impetus to explore for massive sulphide deposits. If the now widely accepted seawater circulation model for submarine massive sulphide deposits is accepted (Franklin and others, *Economic Geology 75th Anniversary Volume*, 485-627, 1981), then high gold contents would be expected in the deposits if the underlying Ordovician rocks were included in the deposit-forming circulation systems. This model is supported by the major new intersection of 15 m massive sulphide averaging 4.88 g/tonne gold at Lewis Ponds near Orange reported in a press release by Tri Origin Exploration Ltd.

For further information, contact D. Wyborn, P.G. Stuart-Smith, D.A. Wallace, or G.A.M. Henderson.



# Sequence stratigraphic interpretation of Bowen and Surat Basin successions, Taroom region, Queensland

The Taroom area of the Bowen and Surat Basins (Fig. 1) is currently being explored for hydrocarbons. This central Queensland area is between latitudes 25° and 26° S and longitudes 149° and 150° 30' E, within the MUNDUBBERA and TAROOM Sheet areas. The region's potential has been indicated by gas shows from stratigraphic plays in the Moolayember Formation near the axis of the Taroom Trough, and from fractured rock reservoirs near the deformed eastern margin of the basin. The studies are designed to provide an integrated sequence stratigraphic and structural framework to aid future exploration.

Preliminary results of the first phase of the Sedimentary Basins of Eastern Australia project have just been released as *BMR Record 1991/102 (Fossil Fuels 7)*, *Sequence stratigraphic interpretation of seismic data in the Taroom region, Bowen and Surat Basins, Queensland*, with a folio of twenty-eight 1:250 000 structure contour and isopach maps (in two-way travel time) of selected horizons and intervals, plus a seismic line location map.

## The project

The National Geoscience Mapping Accord project on the Sedimentary Basins of Eastern Australia is being undertaken by AGSO, the Geological Survey of Queensland, and the New South Wales Department of Mineral Resources, with co-operation from industry, CSIRO, and universities. The aim is an

integrated basin analysis of the Bowen, Gunnedah and Surat Basins with emphasis on their sedimentary, structural, tectonic and thermal histories to assess the economic potential for hydrocarbons.

The geological interpretation of a regional network of seismic lines, acquired by both hydrocarbon exploration companies and AGSO, forms a major contribution to the project. The objectives are: using sequence stratigraphic analysis; determine the spatial and temporal distribution of various stratigraphic packages as an aid towards understanding the distribution and nature of hydrocarbon resources; and determine the structural geometry, evolution and tectonic setting of the sedimentary packages.

## Sequences and sequence boundaries

Several reflectors have been chosen as the framework for seismic interpretation in the Taroom area (Fig. 2), most being within the Permian-Triassic Bowen Basin succession — one is the unconformity between the Bowen and Surat Basins, and two are within the Jurassic Surat Basin succession. Many of the reflectors are sequence boundaries. The seismic data were tied to well data where possible; only seven exploration wells have been drilled and most of the stratigraphic bores are relatively shallow.

The Taroom Trough succession in the Taroom region commences with the thick Camboon Volcanics. The volcanic rocks are overlain by Early-Late Permian marine sediments, the base being a regional sequence boundary (B6). The succeeding two reflectors correspond with the bases of the Flat Top Formation (B26) and Gylanda Formation (B64), using tentative ties with the Cockatoo Creek 1 well. There are some indications (truncation, onlap) that B64 may be a sequence boundary; the correlative boundary has been shown to be a sequence boundary in the Denison Trough to the west through both outcrop and subsurface studies. The base of the Baralaba Coal Measures is usually expressed as a well-marked reflector (B17) at the base of a package of strong reflectors caused by coal seams.

A reflector (B39) equivalent to the sequence boundary at the base of the Freitag Formation in the Denison Trough was identified near the Glenhaughton 1 well on the Comet Ridge in the northeastern part of the Taroom region. We tentatively correlate it with the major unconformity in the Taroom Trough between the Buffel and Oxtrack Formations. In the Taroom Trough, the Buffel Formation is too thin to be resolved seismically, and therefore the B39 sequence boundary is indistinguishable from the underlying B6 reflector.

The Permian succession is overlain by the non-marine latest Permian-Triassic Rewan Group, Clematis Group and Moolayember Formations. The thick Triassic section contains six recognisable genetic sequences, which are characterised by great lateral variability in both the strength and continuity

of reflectors, owing to lateral lithological changes within a largely fluvial assemblage of stacked channel and overbank deposits. This is particularly evident in the Rewan Group where, on several north-south lines, a mounded seismic character, possibly representing alluvial fan deposits, can be seen. Some of the reflectors within the Triassic succession, including some of the sequence boundaries, may be palaeosol horizons, previously reported from the Rewan and Clematis Groups. At the sequence boundary at the base of the Rewan Group (B33), erosional relief is visible on some lines, and underlying strata are truncated in many sections. Of the five reflectors chosen within the Triassic section, all except the intra-Rewan Group reflector (B44) are sequence boundaries. The unconformity at the base of the Clematis Group (B48 reflector) is in places markedly angular and truncates reflectors in the underlying Rewan Group, including the B44 reflector. This angular relationship is more common on the western side of the Taroom Trough, towards the Comet Ridge, reflecting structural movement on the western limb of the Mimosa Syncline prior to the deposition of the Clematis Group. This is consistent with outcrop studies indicating changes in palaeocurrent directions, with the introduction of westerly-sourced currents and more mature quartzose sediment at the beginning of deposition of the Clematis Group. A relatively strong reflector within the Clematis Group (B20) has been tied to the base of the Showgrounds Sandstone in Tiggrigie Creek 1, which is an unconformity farther south in the Trough, but is not recognisable as such in the Taroom area. The remaining two reflectors in the Bowen Basin succession occur at the base of (B46), and within (B10), the Moolayember Formation; both appear to truncate underlying strata on several lines.

The Bowen Basin is overlain unconformably by the generally flat-lying Jurassic-Cretaceous rocks of the Surat Basin. The strong unconformity at the base of the Precipice Sandstone (S22) is the erosion surface formed during the Late Triassic, following a strong compressional event. Spectacular erosional truncation of the uplifted eastern side of the basin is shown on numerous lines. In the axial part of the Trough, the angular discordance is not as great, and in places the reflectors are parallel. Two reflectors have been picked in the overlying sediments. The S7 reflector occurs at the base of a package of relatively strong parallel reflectors that represent the interbedded sandstone and shale of the Evergreen Formation. The S13 reflector may be a maximum flooding surface; it corresponds to the oolitic Westgrove Ironstone Member, a product of widespread chemical sedimentation with little clastic input at a time of marine incursion.

A more detailed sequence stratigraphic analysis, e.g. identifying systems tracts, has not been attempted at this stage. The marine portion of the Permian succession generally occurs deep in the section where data quality is poor, as only low frequency, long-wave-

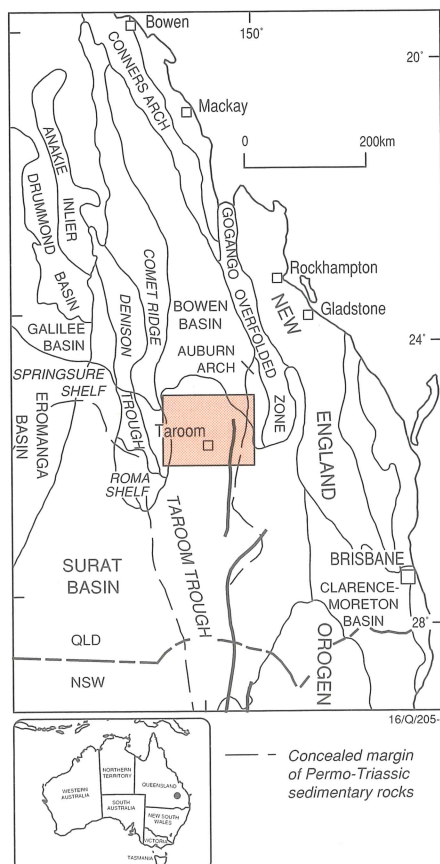


Fig. 1. Location of the Taroom region within the sedimentary basins of eastern Australia.



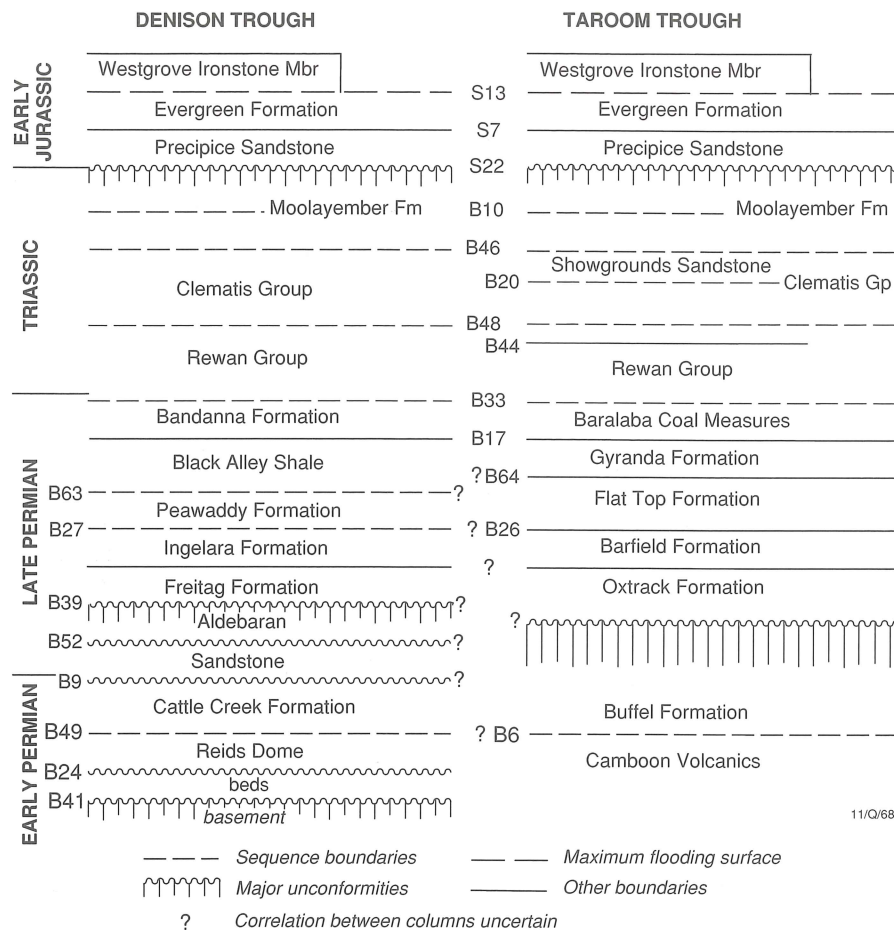


Fig. 2. Stratigraphy of the Taroom region showing the position of sequence boundaries, unconformities, and other reflectors (indicated by code numbers).

length data are recorded. The remainder of the section consists of largely non-marine rocks. Despite some reservations in the literature as to whether, or how, sequence stratigraphic analysis can be applied to non-marine rocks, we have established that at least **major** sequence boundaries can be recognised in fluvial deposits. Nevertheless, discriminating between systems tracts in non-marine sediments is difficult, because the sequences may be more directly controlled by tectonics and sediment supply than by sea-level change. In addition, those sequence boundaries that we have identified in the non-marine section, are probably only a few of the sequence boundaries present, most of which may be very subtly expressed or beyond seismic resolution.

### Geometry of stratigraphic sequences and structural development

A series of structure contour and isopach maps (in two-way travel time) have been compiled using the chosen reflectors. These maps give a better understanding of the distribution of the sedimentary packages and their subsurface configuration. Isopachs of the Permian succession generally show a meridional trend with depocentres commonly developed on the eastern side of the area,

indicating an asymmetric stratigraphic profile. The Triassic section exhibits a similar pattern, except that the geometry of these units has been strongly modified as a result of major uplift and subsequent erosion on the eastern side of the basin. The Surat Basin isopachs show a symmetrical disposition around the south plunging synclinal axis, thinning gradually towards the exposed eroded margins in the north and east.

The structure contour maps depict the major structural features: the near meridionally trending Mimosa Syncline and the monocline in the Bowen Basin succession on the eastern side of the syncline. The monocline possibly was produced by east-directed back-thrusting during major west-directed thrusting at the eastern margin; uplift of the eastern margin was therefore caused by duplexing in a triangle zone below the sedimentary succession.

Analysis of the structural geology and tectonic subsidence curves has allowed a reconstruction of the history as follows:

- Eruption of a thick volcanic pile during an initial thermal event.
- Initial subsidence driven by cooling and thermal relaxation, which continued for about 10 m.y. after cessation of volcanism in the east, and for 20 m.y. in the west.
- Rapid subsidence driven by foreland

loading. This commenced in the Early Permian, continuing until the Middle Triassic, and resulted in an asymmetric basin with about 7 km of fill; there was a time lag of about 10 m.y. for the effects of thrusting to be propagated 100 km to the west.

- Cessation of sedimentation after deposition of the Moolayember Formation — caused by uplift of the eastern margin due to the westward advance of thrust sheets.
- A 40 m.y. period of non-deposition and erosion.
- Slow subsidence driven by thermal relaxation due to cooling of the lithosphere, recommenced in the Jurassic.

For further information, contact Jennie Totterdell, Albert Brakel, Allan Wells or Russell Korsch (Onshore Sedimentary & Petroleum Geology Program) at AGSO.

## The magnetic anomaly map of Australia

The compilation of the magnetic map of Australia is at present in its final stage. The airborne magnetic land surveys have been routinely conducted since 1951. Over four million kilometres have been flown, covering the majority of land with so-called reconnaissance surveys at 1500–3200 m line spacing, at a flying height of 150 m.

Located profile data for these surveys have been regridded to 15 second of arc (about 400 m); subsequently merged on a 1:250 000 sheet basis by minimizing and smoothing the discrepancies between data from adjacent surveys.

The resulting maps contain reliable short-wavelength information of an order of 60 km or less, which is attributable to the surface and near-surface geology.

The final map provides a useful synoptic view of magnetic anomaly patterns, expected to give an important new insight into the geology and tectonics of Australia at continental scale. The map is particularly useful when combined with geological information and other geophysical data, as for example radiometrics.

The aeromagnetic data in the form of 15 second of arc grid are easily accessible on the IIS processing system, and any particular area can be windowed according to the needs of the user.

A poster showing progress with the Australian compilation will be presented at the 9th ASEG Geophysical Conference and Exhibition, 5–8 October 1992, Gola Coast, Queensland.

The final map is expected to be published in December 1992.

For further information, please contact Dr C. Tarlowski, AGSO, Airborne Group.